The Plant Cell, Vol. 16, 3197–3215, December 2004, www.plantcell.org © 2004 American Society of Plant Biologists

RESEARCH ARTICLES

Characterization of Antirrhinum Petal Development and Identification of Target Genes of the Class B MADS Box Gene *DEFICIENS* [W]

Melanie Bey,[a] Kurt Stüber,[a] Kurt Fellenberg,[b] Zsuzsanna Schwarz-Sommer,[a] Hans Sommer,[a] Heinz Saedler,[a] and Sabine Zachgo[a,1]

[a] Department for Molecular Plant Genetics, Max Planck Institute for Plant Breeding Research, 50829 Cologne, Germany
[b] Department of Functional Genome Analysis, German Cancer Research Center, 69009 Heidelberg, Germany

The class B MADS box transcription factors *DEFICIENS* (*DEF*) and *GLOBOSA* (*GLO*) of *Antirrhinum majus* together control the organogenesis of petals and stamens. Toward an understanding of how the downstream molecular mechanisms controlled by *DEF* contribute to petal organogenesis, we conducted expression profiling experiments using macroarrays comprising >11,600 annotated Antirrhinum unigenes. First, four late petal developmental stages were compared with sepals. More than 500 ESTs were identified that comprise a large number of stage-specifically regulated genes and reveal a highly dynamic transcriptional regulation. For identification of *DEF* target genes that might be directly controlled by *DEF*, we took advantage of the temperature-sensitive *def*-101 mutant. To enhance the sensitivity of the profiling experiments, one petal developmental stage was selected, characterized by increased transcriptome changes that reflect the onset of cell elongation processes replacing cell division processes. Upon reduction of the *DEF* function, 49 upregulated and 52 downregulated petal target genes were recovered. Eight target genes were further characterized in detail by RT-PCR and in situ studies. Expression of genes responding rapidly toward an altered *DEF* activity is confined to different petal tissues, demonstrating the complexity of the *DEF* function regulating diverse basic processes throughout petal morphogenesis.

INTRODUCTION

The regulation of floral organogenesis has been intensively studied during the last 15 years by analyzing floral homeotic mutants. Based on single and double mutant phenotypes from *Antirrhinum majus* and *Arabidopsis thaliana*, a simple ABC model was established that explains how three groups of regulatory genes act in a combinatorial manner to specify floral organogenesis. Isolation of these key floral regulatory genes showed that they are mainly representing MADS box transcriptions factors (reviewed in Lohmann and Weigel, 2002; Jack, 2004). In Antirrhinum, two homeotic genes *DEFICIENS* (*DEF*; Sommer et al., 1990; Schwarz-Sommer et al., 1992) and *GLOBOSA* (*GLO*; Tröbner et al., 1992), the so-called class B genes, control petal and stamen organogenesis. Their RNA and protein expression patterns overlap and are maintained until late stages of petal and stamen development (Zachgo et al., 1995). The *def* and *glo* mutants show identical phenotypes, with petals transformed into sepaloid organs and stamens transformed into carpeloid structures. Additionally, initiation of carpel organogenesis in the center of the flower is dependent on *DEF* and *GLO* function because no fourth whorl organs are formed in the respective mutants. The DEF and GLO proteins heterodimerize and were shown to bind in vitro as dimers to short conserved DNA elements, called CArG-boxes (Schwarz-Sommer et al., 1992; Tröbner et al., 1992). CArG-box elements are also located in their own promoters and are presumed to mediate maintenance of late expression by an autoregulatory mechanism (Schwarz-Sommer et al., 1992; Zachgo et al., 1995). The DEF/GLO heterodimer associates with the MADS box protein SQUAMOSA via their C termini, resulting in an increased DNA binding affinity. This ternary complex requires for binding the presence of two CArG-boxes, located, for instance, in the *GLO* promoter (Egea-Cortines et al., 1999).

Although class B genes from Antirrhinum and various other species have been intensively studied, still little is known about the target genes that realize their regulatory potential during petal and stamen organogenesis. A modest number of putative class B target genes that are preferentially expressed either in petals or stamens was isolated by differential screening strategies from Antirrhinum, Arabidopsis, and *Gerbera hybrida* (Nacken et al., 1991a, 1991b; Rubinelli et al., 1998; Sablowski and Meyerowitz,

[1] To whom correspondence should be addressed. E-mail szachgo@mpiz-koeln.mpg.de; fax 0049-221-5062113.
The author responsible for distribution of materials integral to the findings presented in this article in accordance with the Instructions for Authors (www.plantcell.org) is: Sabine Zachgo (szachgo@mpiz-koeln.mpg.de).
[W] Online version contains Web-only data.
Article, publication date, and citation information can be found at www.plantcell.org/cgi/doi/10.1105/tpc.104.026724.

1998; Kotilainen et al., 1999). In vivo proof for direct regulation of *NAP* (for *NAC-LIKE*, *ACITVATED BY AP3*/*PI*) by the Arabidopsis class B protein APETALA3 (AP3; Jack et al., 1992) was delivered by an engineered steroid-inducible *AP3* system (Sablowski and Meyerowitz, 1998). *NAP* was proposed to participate in the transition from cell division to cell elongation processes in petals and stamens.

Recently, several studies were performed using high-throughput genomic approaches to characterize flower development in roses, Arabidopsis, and *Iris hollandica* (Channelière et al., 2002; Guterman et al., 2002; Schmid et al., 2003; van Doorn et al., 2003; Zik and Irish, 2003; Wellmer et al., 2004). Arabidopsis expression profiling studies were performed with probes from different floral mutant inflorescences to identify petal- and stamen-specific genes. The number of the identified genes that depend on the activity of the Arabidopsis class B genes *AP3* and *PISTILLATA* (*PI*; Goto and Meyerowitz, 1994) throughout petal and stamen development varies between ~200 and 1100 (Zik and Irish, 2003; Wellmer et al., 2004). Antirrhinum petals served as a key model system to analyze flower asymmetry, scent, and pigmentation production as well as epidermal cell differentiation leading to conical cell formation contributing to their velvet sheen (Noda et al., 1994; Luo et al., 1999; Dudareva et al., 2000). Whereas growth of early petal stages has been reported from different species to be realized by cell division processes, later growth is mainly achieved by cell elongation (Martin and Gerats, 1993; Ben-Nissan and Weiss, 1996; Roll-and-Lagan et al., 2003). These examples illustrate that the formation of different tissues with distinctive functions requires a tight spatial and temporal regulation that is likely reflected by dynamic transcriptome changes throughout petal organogenesis. A better understanding of organ formation would thus profit from a temporally and spatially restricted target gene analysis to avoid blurring of differences in mRNA expression levels. The large size of the Antirrhinum flower allows analysis of dissected stages and organs. Moreover, Antirrhinum offers a large flower mutant collection, forward and reverse genetic tools, and a molecular linkage map, and very recently a large EST collection has been established (for a review, see Schwarz-Sommer et al., 2003).

Here, we present an Antirrhinum genomics approach using macroarrays with >11,600 spotted Antirrhinum unigenes. Toward a better understanding of the molecular mechanisms controlled by *DEF* during petal organogenesis, we conducted a two-step profiling procedure. First, late petal and sepal development was compared. Class B gene expression in sepals conditions petal organ fate, as shown by the class B mutant phenotypes and by ectopic petal formation in the first whorl upon class B overexpression (Sommer et al., 1990; Davies et al., 1996). More than 500 ESTs were identified representing target genes directly and indirectly controlled by *DEF*. For determination of more directly controlled target genes, profiling experiments were conducted with petals from the conditional *def*-101 mutant. More than 100 upregulated and downregulated *DEF* petal target genes were identified. Further expression analyses of selected target genes corroborated their dependence on the *DEF* function and reflect the broad spectrum of basic cellular processes contributing to petal development.

RESULTS

The Conditional *def*-101 Mutant: A Tool to Identify *DEF* Target Genes

Differences in the temporal and quantitative requirement of the *DEF* function during early flower development were investigated using the temperature-sensitive *def*-101 mutant (Zachgo et al., 1995). Flowers of *def*-101 mutants cultivated at the permissive temperature (15°C) display an almost wild type–like morphology, with upper and lower lopes being slightly reduced in size and less strongly folded (Figures 1A and 1B). *Def*-101 plants grown at the nonpermissive temperature (26°C) resemble *DEF* null-mutants (Figure 1C). Higher temperature was shown to affect the stability of the DEF/GLO heterodimer, causing its rapid degradation and thus made the *def*-101 mutant an ideal tool for target gene identification.

To analyze different late petal stages by expression profiling experiments, we conducted *def*-101 temperature-shift experiments to determine until which stages reduction of *DEF* function still causes morphologically visible effects. *Def*-101 plants were grown at the permissive temperature until the oldest bud reached a size of ~1 cm (defined as stage 3, see below) and were then grown until anthesis at the nonpermissive temperature. Figure 1D shows a wild type–like *def*-101 flower before reduction of the *DEF* function. At this stage, all floral organs are formed and stamens already developed microspores and are about to reach their final length by filament elongation. After 4 d of cultivation at the nonpermissive temperature, carpeloid structures were formed close to the base of the filaments (arrows in Figure 1E), and petal development is disturbed. In comparison with *def*-101 plants cultivated exclusively in the cold (Figure 1F), reduction of the *DEF* function for 72 h affected coloration and shape of petals. For instance, formation of greenish sectors was observed, indicating loss of petal identity and transformation toward sepaloid organs (Figure 1G). The shortest time span of *DEF* function sufficient to restore a morphological aspect of *DEF* control was determined by double shift experiments. Plants were grown at the nonpermissive temperature, and plants with ~1-cm-long inflorescences were shifted transiently for 12, 24, 48, and 72 h to the permissive temperature before cultivation until flower maturation at the nonpermissive temperature. Transient activation of the *DEF* function for 24 h was sufficient to regulate downstream targets that control meristematic activities in the center of the flower, such that one flower per investigated inflorescence initiated a normal fourth whorl (Figure 1H). By contrast, second and third whorl organs stayed transformed, even after extended periods of *DEF* upregulation for 72 h (data not shown). Thus, an early and transient *DEF* function is required to initiate fourth whorl development that subsequently does not depend on *DEF* activity. By contrast, a continuous *DEF* function is required until late stages to maintain normal petal and stamen differentiation. These observations emphasize the importance of conducting spatio-temporal-specific studies to identify target genes involved in different regulatory processes. We took advantage of the large Antirrhinum flower and used petal organs from distinct stages to analyze late stages of petal morphogenesis and to identify the genes that realize the regulatory potential of *DEF*.

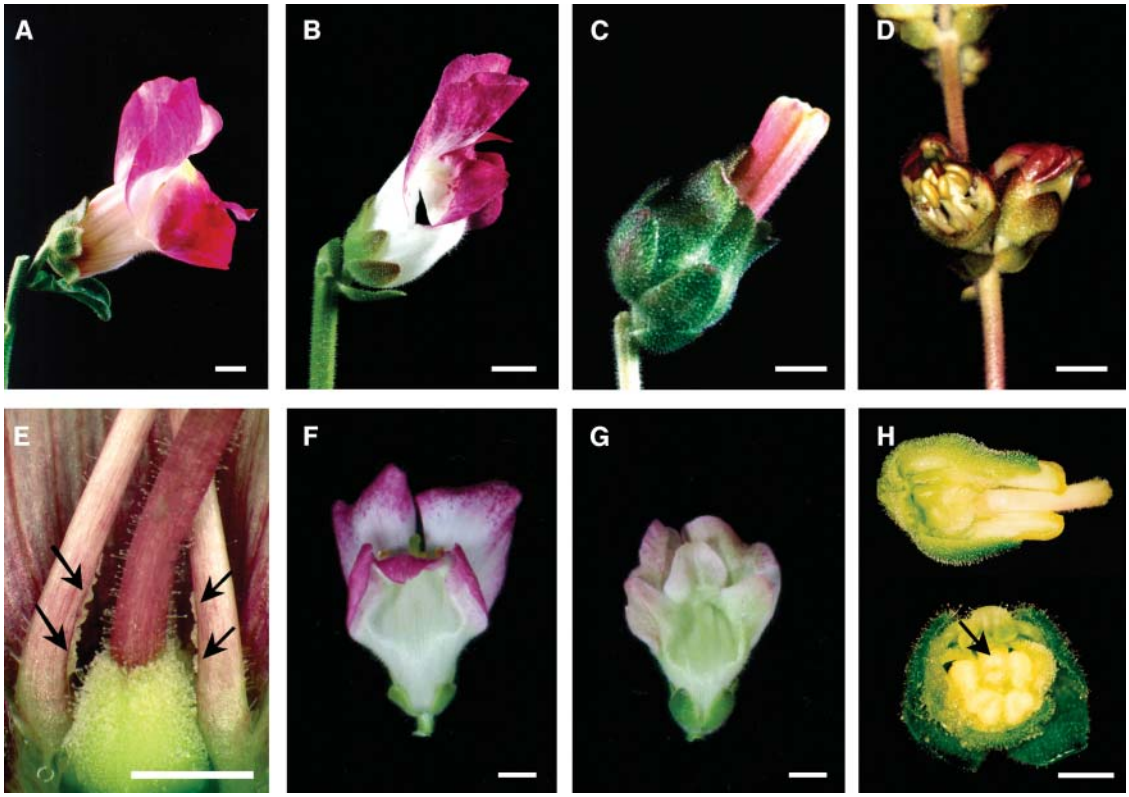

Figure 1. Effects of an Altered *DEF* Function during *def*-101 Floral Development.

(A) Mature Antirrhinum wild-type flower.
(B) and **(C)** Morphology of a mature *def*-101 flower grown at the permissive temperature (15°C) and nonpermissive temperature (26°C), respectively.
(D) *Def*-101 flowers grown until a length of ~1.0 cm at 15°C. Petals were removed from one flower to show stamens.
(E) *Def*-101 flower, cultivated at 15°C until a bud size of ~1.0 cm had formed, and then transferred to 26°C for 4 d. Reduction of *DEF* function caused formation of ovule-like structures close to the base of the mature filaments (marked with arrows).
(F) Ventral view from a mature *def*-101 flower cultivated at the permissive temperature (15°C).
(G) Ventral view from a *def*-101 flower grown at the permissive temperature until a size of 1.0 cm and then cultivated for 3 d at the nonpermissive temperature.
(H) Phenotypic response to transient activation of the *DEF* function for 24 h. *Def*-101 flowers were cultivated at 26°C until an early stage when sepal primorida were just initiated (defined as described in Zachgo et al., 1995). After a transient activation of the *DEF* function for 24 h at 15°C, final maturation occurred at 26°C. In the top flower, first and second whorl organs were partially removed to reveal transformed third whorl organs enclosing restored fourth whorl carpels. The bottom picture shows a transverse section through an identically treated *def*-101 flower. Arrow marks carpels in the fourth whorl.
Bars in **(A)** to **(H)** = 0.5 cm.

Characterization of Late Petal Development in Antirrhinum by Expression Profiling

Macroarrays were produced by spotting 14,186 Antirrhinum ESTs representing 11,615 partially sequenced unigenes from different vegetative and floral organs as double spots on nylon filters. The array filters represent ~40% of the estimated total Antirrhinum cDNA number, assuming that the number of expressed genes is comparable between Arabidopsis and Antirrhinum.

First, we characterized petal development by comparing sepal and petal transcriptomes. By this approach, all identified differentially expressed ESTs represent genes whose transcription is directly or indirectly controlled by the DEF/GLO proteins. To increase the sensitivity and resolution, late petal development was divided into four distinct stages (Figures 2A and 2B). In stage 1 (bud length 0.5 to 0.8 cm), petals are still enclosed by sepals, whereas stage 2 (0.8 to 1.0 cm) is characterized by an outgrowth of petals. At stage 3 (1.0 to 2.0 cm), rapid growth of the flower starts, reflected by doubling flower length within 3 d. During stage 4 (2.0 to 4.0 cm), final growth until anthesis of the flower is realized. Petal stages 1 and 2 match the late phase F and stage 3 and 4 the phase G, which were recently defined when a temporal and morphological framework was established for the entire Antirrhinum flower development (Vincent and Coen, 2004). Petal tissue from the four stages was harvested separately. Sepals were pooled and used as one sample for comparison as no

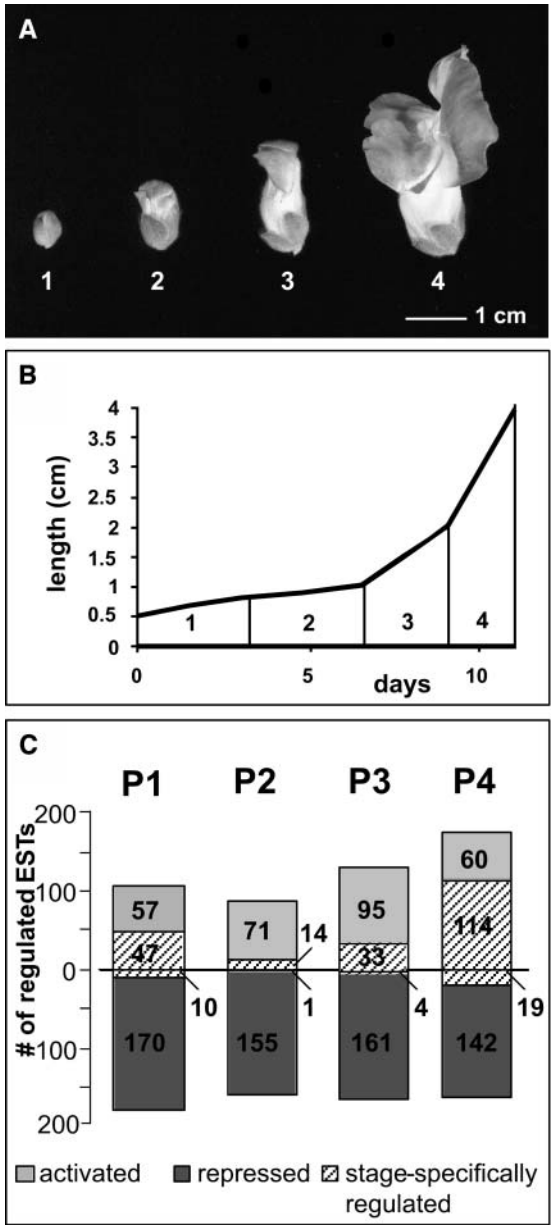

Figure 2. Transcriptome Dynamics during Antirrhinum Petal Development.

(A) Division of late petal development into four stages.

(B) Increase in bud length through stages 1 to 4.

(C) ESTs differentially expressed between sepals and petals from stages 1 to 4. Numbers indicate activated and repressed ESTs, and hatched lines mark the number of ESTs that are differentially regulated exclusively in the respective stage.

morphological differences affecting, for example, their size or trichome development could be observed during the analyzed stages.

To ensure the reliability of the results, hybridizations were repeated three times using at least two biological RNA samples for probe preparation. Signal intensities on filters hybridized with radioactively labeled probes were determined and further processed with the multi-conditional hybridization intensity processing system (M-CHiPS; Fellenberg et al., 2002). After normalization for each gene and experimental condition, the median of the data was calculated, and the significance of variations in RNA levels was assessed (Beissbarth et al., 2000; Fellenberg et al., 2001; see Methods for details). Quality of the data sets was further controlled by determination of the Pearson correlation coefficient, revealing good reproducibility among individual filters in the same experiment (Figures 3A and 3B). Gradual reduction of the coefficient values for the individual experimental comparisons reflects increased transcriptome differences throughout the investigated stages (Figures 3C to 3F).

The used data processing system has been shown to detect subtle but significant transcriptional changes and meets the criteria that were recently established for international standardization and quality control of array experiments at the MIAME convention (Brazma et al., 2001; Lagorce et al., 2003). Independent expression analyses were conducted, confirming that a cutoff value of 1.2-fold change can be reliably applied in this data set for an intensity range that disregards 80% of the spotted genes as not expressed (Figure 6; see supplemental data online). Using this value, 537 ESTs were identified as being differentially expressed between sepals and petals in at least one stage during late flower development (see supplemental data online for list of all genes). This number of ESTs includes up to 22% of genes that were spotted twice on the filter. Figure 2C shows the numbers of ESTs differentially expressed between sepals and the four petal stages. Additionally, numbers of stage-specifically regulated ESTs are indicated. Counting all the activated and repressed nonredundant ESTs revealed 226 repressed and 322 activated ESTs (data not shown). Expression of 45% of the ESTs (104/226) is constantly reduced throughout late petal development, and only 15% of the ESTs (34/226) are repressed specifically during one developmental stage.

By contrast, dynamic expression changes were observed for the genes activated during petal development. Only ~3% of the ESTs (11/322) are expressed significantly higher throughout all petal stages compared with sepals, whereas 60% (208/322) are upregulated exclusively during one petal stage (Figure 2C). The high value of 104 ESTs, activated in stage 1, includes 47 stage-specifically regulated ESTs and probably reflects the sampling. Because petals younger than stage 1 were not separately analyzed, transcript changes in stage 1 might have accumulated. After stage 1, the number of activated ESTs gradually increases from 85 (stage 2) to 128 (stage 3), and finally up to 174 (stage 4), coinciding with a steady increase in the proportion of the stage-specific ESTs. Whereas the contribution of the stage-specifically regulated genes in stage 2 is only ~16% (14/85), this increases during stage 3 up to ~26% (33/128) and, most strongly, up to ~66% (114/174) during stage 4. By contrast, only <1% (1/156, stage 2), 3% (4/165, stage 3), and 13% (19/161, stage 4) are stage-specifically downregulated, indicating a higher uniformity of the repressed transcription mode compared with the activated mode.

In summary, these data reveal a highly dynamic gene expression regulation, with a large proportion of transcripts being

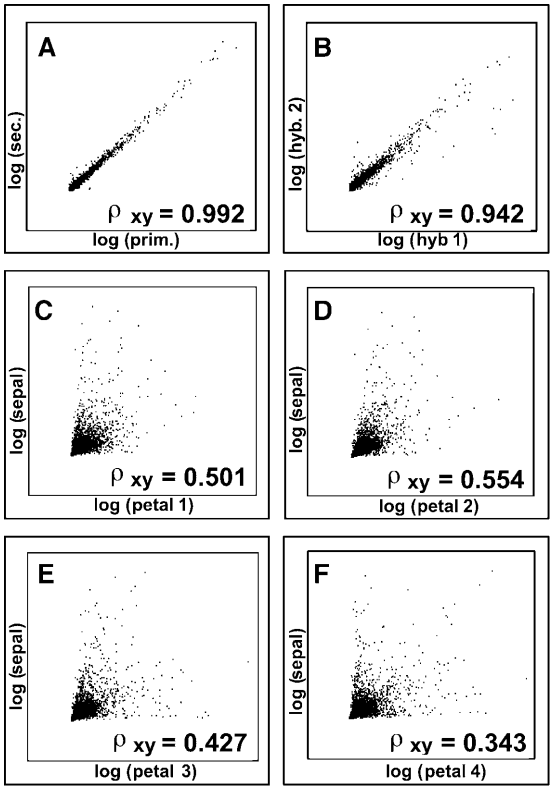

Figure 3. Evaluation of Macroarray Data Analysis.

Scatterplot and Pearson correlation coefficients are shown for data quality assessment. Values close to 1.0 reflect a high degree of linear relationship between the compared data sets, whereas decreasing coefficient values indicate the extent of differential expression.
(A) Signal intensity comparison of primary and secondary spot replicates from a single representative hybridization assures high filter quality.
(B) Representative comparison of two hybridizations using probes from petals at stage 3 demonstrates high reproducibility.
(C) to **(F)** Scatterplot and coefficient of median intensities from three independent hybridizations per condition. Petal stages 1 to 4 were compared with sepals. Progression through petal organogenesis coincides with decreasing coefficients, reflecting accumulation of transcriptome changes.

stage-specifically upregulated by *DEF* during late stages of Antirrhinum petal development.

Functional Annotation of Regulated Genes during Petal Development

To determine putative functions of differentially expressed cDNAs, Antirrhinum EST sequences were functionally annotated. A surrogate annotation approach was conducted, using as a basis the existing role categorization from the Munich Information Center for Protein Sequences (MIPS) available for the proteome of Arabidopsis. This commonly applied approach is based on the assumption that conserved sequences reflect functional relationships. Antirrhinum genes with an expect value (E-value) of $<2.0\ E^{-12}$ were grouped into 20 functional categories. Applying this E-value, no homolog could be identified for 36% (4226 genes) of the unigene set, and we assume that this group might comprise genes exerting functions specific for Antirrhinum. They were not included in a functional comparison conducted with the Arabidopsis unigene set (see Methods). Distribution of genes among the different groups is very similar between the two species (Figure 4), indicating that the Antirrhinum EST collection comprises a representative proportion of the totally expressed genes.

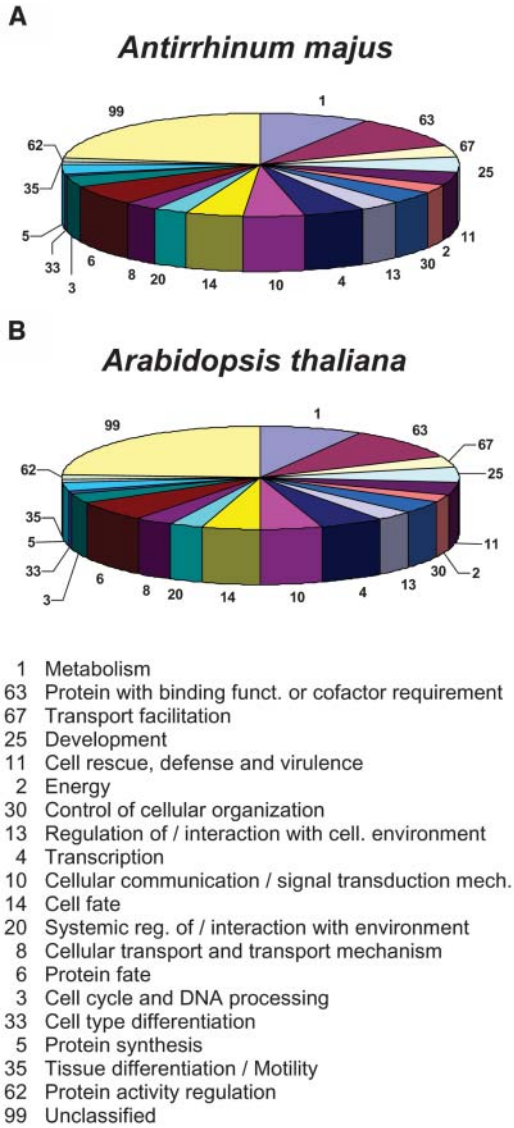

Figure 4. Functional Classification of Antirrhinum and Arabidopsis Unigenes.

Unigenes from Antirrhinum and Arabidopsis were classified into 20 functional categories and numbered according to MIPS.
(A) Antirrhinum gene functions were assigned through annotation to Arabidopsis without considering genes for which no homolog could be identified.
(B) Arabidopsis unigene categorization.

Table 1. Comparison of Functional Categories throughout Wild-Type Petal Development

Functional Category	Percentage of ESTs Regulated								Percentage of ESTs Expressed in Petals ($n = 2.851$)	Percentage of ESTs Represented on Array ($n = 14.186$)
	in P1 ($n = 275$)	Only in P1 ($n = 57$)	in P2 ($n = 241$)	Only in P2 ($n = 15$)	in P3 ($n = 284$)	Only in P3 ($n = 37$)	in P4 ($n = 333$)	Only in P4 ($n = 124$)		
Metabolism	30	21	32	33	36	41	38	43	27	15
Protein with binding function or cofactor requirement	27	35	26	33	27	43	20	17	30	17
Transport facilitation	13	2	15	13	16	19	15	14	12	6
Development	12	14	13	33	14	27	11	11	15	8
Cell rescue, defense, and virulence	14	12	15	27	17	16	17	18	13	7
Energy	14	4	15	20	17	14	18	13	11	5
Control of cellular organization	12	25	10	27	12	30	9	13	12	6
Regulation of/interaction with cellular environment	12	11	13	27	13	19	10	6	10	5
Transcription	12	14	10	13	11	14	10	10	13	9
Cellular communication/signal transduction mechanism	11	18	12	33	11	16	11	9	12	9
Cell fate	11	19	10	7	10	27	7	9	14	8
Systemic regulation of/interaction with environment	7	7	10	20	10	8	10	15	9	5
Cellular transport and transport mechanism	7	2	7	0	7	5	6	5	7	5
Protein fate	16	25	15	27	12	16	9	10	18	11
Cell cycle and DNA processing	11	23	7	0	7	8	6	2	8	5
Cell type differentiation	2	2	2	7	3	3	4	6	3	1
Protein synthesis	9	18	7	13	6	14	6	8	10	4
Tissue differentiation/motility	2	0	3	7	4	5	5	6	3	1
Protein activity regulation	6	9	5	7	6	8	3	2	4	3
Unclassified	50	60	49	73	54	46	52	72	56	41
Homolog not found	2	4	6	7	2	5	5	2	3	35

Antirrhinum ESTs were classified into 20 functional categories following the role categorization from MIPS. Sums exceeding 100% are a result of possible clustering of one gene into multiple categories. Calculation of percentages was performed for the total number of ESTs regulated during one stage and for exclusively regulated ESTs during one stage. For comparison, percentage frequencies of the whole Antirrhinum EST collection are shown. P1, P2, P3, and P4 represent petal stages 1, 2, 3, and 4, respectively.

For further characterization of petal development, percentages of regulated ESTs within the 20 functional categories were determined (Table 1). Comparison of the resulting numbers with the general representation rate of ESTs in the Antirrhinum EST collection supports highly dynamic gene regulation during petal development. In stage 1, the category cell cycle and DNA processing is overrepresented, but descends to an average percentage at stage 2. Detailed analysis revealed that genes indicative for cell division processes, like histones 2A, 2B, and 4, are particularly dominant in the group of upregulated ESTs during stage 1 (see supplemental data online). Once flowers reach a length of 0.8 cm, the importance of cell division processes to contribute to cell growth ceases, corroborating earlier observations (Martin and Gerats, 1993; Rolland-Lagan et al., 2003).

In an overall comparison (Table 1), the category metabolism is most significantly upregulated throughout all petal stages. Especially, expression of stage-dependently regulated ESTs increases strongly during stages 3 and 4. This might reflect the rapid need of metabolites during the final growth phase of the flower. The proportion of ESTs exclusively regulated during stage 3 starts to increase for a large number of additional categories comprising proteins with binding function, transport facilitation, development, control of cellular organization, and cell fate. Commencing at stage 3 and continuing until stage 4, detailed analysis identified a large group of coregulated ESTs that exert functions associated with cell wall metabolism (see supplemental data online). Identified genes code for enzymes like pectinacetylesterase, modifying cell wall components or structural cell wall proteins, such as extensin-like proteins, a subfamily of hydroxyproline-rich glycoproteins (HRGPs) that are presumed to determine physical characteristics of the plant cell wall (Carpita and Gibeaut, 1993; Knox, 1995; Cassab, 1998). Identification of aquaporins, water channel proteins, and tonoplast intrinsic proteins reflects changing turgor conditions in growing petal cells. Interestingly, the frequency of the unclassified protein group increases throughout petal development. Whereas the available EST set includes 41% of unclassified ESTs, 56% of the ESTs belonging to this group are expressed in petals, and even higher percentages were identified as being stage-specifically expressed. This suggests that a large proportion of genes with a tight expression regulation during petal development exert an intriguing, yet uncharacterized, function during petal morphogenesis.

The major group of ESTs that are continuously repressed in developing petals are related to photosynthesis, like ribulose-1,5-bisphosphate carboxylase/oxygenase (Rubisco) small

chain, Rubisco activase, and a light harvesting chlorophyll *a*/*b* binding protein precursor (see supplemental data online). This is in accordance with the observation that loss of the *DEF* function at late petal stages still causes activation of the photosynthetic program as indicated by the observed regreening of second whorl organs (Figure 1G).

Identification of *DEF* Target Genes

Further profiling experiments were conducted with the *def*-101 mutant to identify genes that are more likely to represent direct targets of the DEF/GLO heterodimer as their expression level is altered upon abolishing the *DEF* function for different time spans. Petal stage 3 was selected for this target gene screen because the number of novel, stage-specifically upregulated genes increases at this stage, and the *DEF* function was shown to be still required to maintain normal petal morphogenesis. For petal probe preparation, *def*-101 plants grown at the permissive temperature until stage 3 were shifted for 0, 24, and 72 h to the nonpermissive temperature. Parallel experiments were performed with wild-type flowers to exclude temperature-sensitive genes from the studies (shown in supplemental data online).

Expression of 125 ESTs was significantly changed after reducing the *DEF* function for 24 and/or 72 h. Seventeen ESTs needed to be subtracted because they represented generally temperature-sensitive genes. The resulting EST number of 108 represents 101 unigenes, comprising 67 genes that were already recovered by the petal/sepal comparison. Forty-nine genes were identified as downregulated upon *DEF* reduction, thus representing activated target genes. A nearly equal proportion of 52 genes was upregulated and thus forms the group of repressed genes. Table 2 shows the relation between the representation of genes in the EST collection with those that are expressed in petals at stage 3 and with those specifically regulated in this stage. Ten of the 20 considered categories show similar percentages in all three data sets. In seven categories, target genes are overrepresented, most significantly in the groups metabolism, transport facilitation, energy, and control of cellular organization. As already revealed by the sepal/petal comparison, these data emphasize the diversity of *DEF* target gene regulation, including a large number of unclassified proteins with putative novel functions during petal morphogenesis.

Furthermore, because the *def*-101 flowers cultivated in the permissive temperature were not fully identical to wild-type flowers, we also conducted a comparison between *def*-101 and wild-type petals at stage 3, both harvested from plants cultivated in the permissive temperature. This revealed that 87 ESTs are differentially regulated, including almost 50% of genes (39/87 ESTs) that show the same tendency of regulation upon reduction of the *DEF* function in the *def*-101 petal stage 3 shift experiments. Out of these, 15 ESTs revealed expression changes >1.2 in the *def*-101 experiments (see supplemental data online). ESTs that were not also identified with the *def*-101 shift experiments might represent target genes that depend on the high level of *DEF* activity reached in wild-type but not in *def*-101 mutant flowers cultivated at the permissive temperature.

Table 2. Functional Assessment of *DEF* Target Genes

Functional Category	Percentage of Genes Regulated in P3 ($n = 101$)	Percentage of ESTs Expressed in P3 ($n = 2.851$)	Percentage of Genes Represented on Array ($n = 11.615$)
Metabolism	38	29	17
Protein with binding function or cofactor requirement	21	31	20
Transport facilitation	19	12	7
Development	18	15	9
Cell rescue, defense, and virulence	16	12	8
Energy	17	12	6
Control of cellular organization	17	12	7
Regulation of/interaction with cellular environment	14	11	6
Transcription	12	14	10
Cellular communication/ signal transduction mechanism	12	12	10
Cell fate	10	15	9
Systemic regulation of/ interaction with environment	10	9	6
Cellular transport and transport mechanism	10	8	5
Protein fate	8	19	13
Cell cycle and DNA processing	8	9	6
Cell type differentiation	5	3	2
Protein synthesis	4	9	6
Tissue differentiation/motility	4	3	2
Protein activity regulation	2	4	3
Unclassified	63	62	45
Homolog not found	5	3	36

Calculations for regulated genes identified by expression profiling experiments with *def*-101 petals from stage 3 were performed with the Antirrhinum unigene data set. For comparison, percentages of ESTs generally expressed at petal stage 3 and represented in the EST database are shown. Sums exceeding 100% are a result of possible clustering of one gene into multiple categories.

Analysis of Activated and Repressed Target Genes

For a more detailed analysis, hierarchical clustering with the 101 target genes was performed (Figure 5). After reducing the *DEF* function for 24 h, the expression of 46 genes was significantly altered. The expression of 27 genes was upregulated and that of 19 genes downregulated. After 72 h, 93 genes were identified (45 upregulated and 48 downregulated). Out of these genes, 20 and 17 revealed a continuous upregulated and downregulated expression, respectively. Among the activated genes, we found two transcription factors (Figure 5A). After reducing the *DEF* function for 24 h, *DEF* expression was significantly decreased, caused by an ongoing autoregulatory control at this late stage (Zachgo et al., 1995). The other transcription factor also represents a MADS box

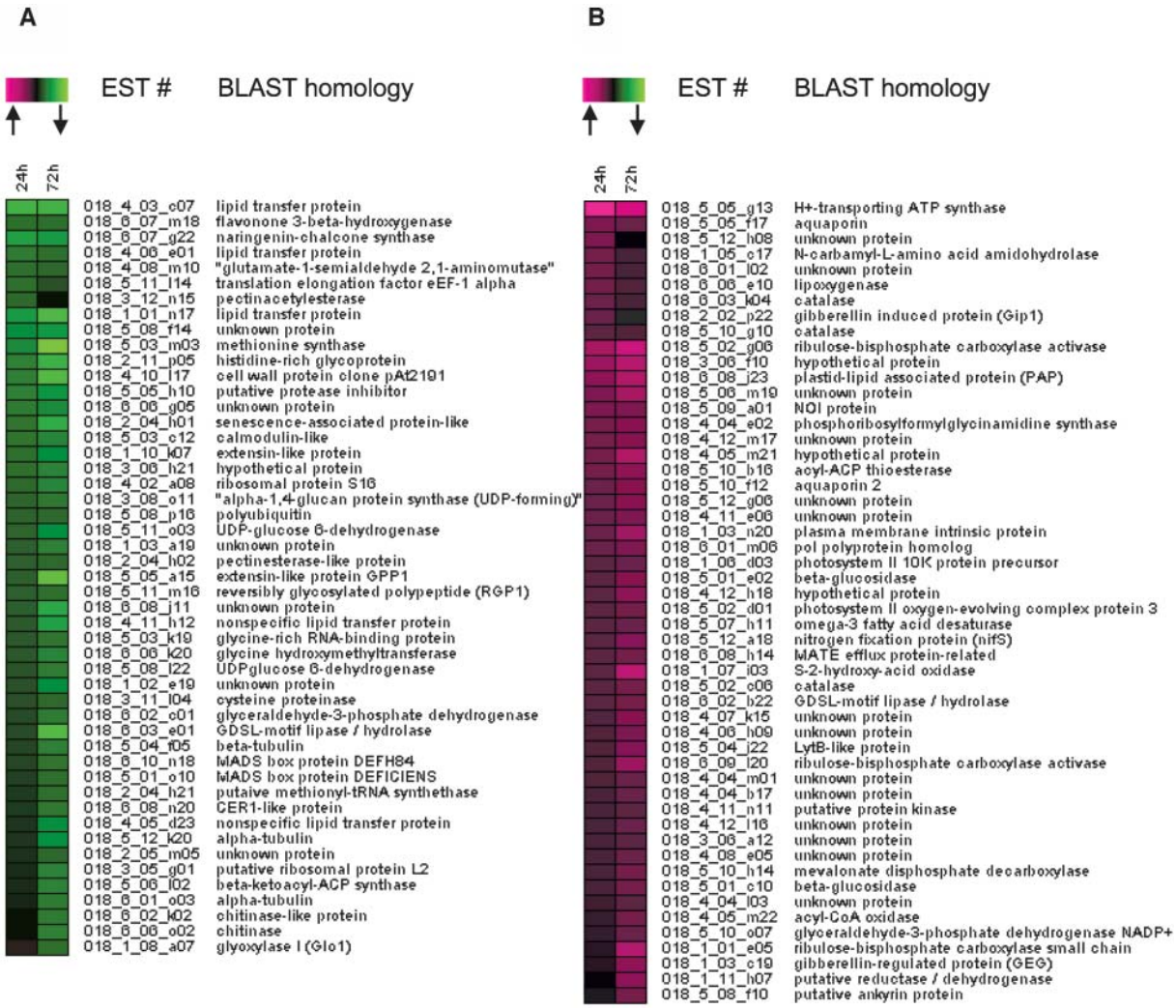

Figure 5. Hierarchical Clustering of Target Genes Regulated by *DEF* in Petals from *def*-101 Flowers at Stage 3.

Median, $\log_2$ transformed intensity ratios of genes significantly regulated by an altered *DEF* function in at least one experimental condition (24 and/or 72 h) were used for hierarchical clustering. Green and magenta represent downregulated and upregulated genes, respectively.

(A) Target genes with a downregulated expression level upon an abolished *DEF* function represent activated *DEF* target genes.

(B) Reciprocally, target genes with an upregulated expression level upon an abolished *DEF* function represent repressed *DEF* target genes.

gene, named *DEFICIENSHOMOLOG84* (*DEFH84*), predominately expressed in petals and stamens of flowers at stage 3 (S. Zachgo, unpublished data). Given that the overall representation of the functional category transcription in the sepal/petal stage 3 comparison experiments was normal (Table 1), we assume that low recovery of transcription factors in the temperature shift experiments is not because of a sensitivity problem of the detection method. Rather, it indicates that *DEF* might control a broad variety of downstream target genes directly without establishing intermediate regulatory modules. A similar observation was reported for *AP3* activity during petal development (Zik and Irish, 2003).

A group of *DEF*-controlled genes is associated with cell wall related processes, overlapping with genes identified in the sepal/petal comparison, like pectinacetylesterases and extensin-like proteins. Another group exerting a rapid expression response comprises cytoskeleton proteins such as α- and β-tubulins that form microtubules (Mayer and Jürgens, 2002). Four different lipid transfer proteins (LTPs), known to mediate the transfer of phospholipids between membranes in vitro (Zachowski et al., 1998), were identified, of which the LTP 018_4_03_c07 responded most strongly toward a reduced *DEF* function. The expression level of two chitinases decreased after reducing the *DEF* function for 72 h. Chitinases are enzymes capable of cleaving chitin,

a major cell wall constituent of many pathogenic fungi (Davis and Bartnicki-Garcia, 1984), and are thought to mediate disease resistance to chitin containing pathogens. Because their expression response occurred with delay, chitinases are probably not directly controlled by *DEF*.

A group of photosynthesis related genes (Rubisco small chain, Rubisco activase, and photosystem II precursor proteins) identified as being repressed in petals by the sepal/petal comparison was upregulated upon reduction of the *DEF* function (Figure 5B). Rubisco activase expression especially responded strongly and rapidly to an altered *DEF* function. This observation is in accordance with the morphological consequences of late reduction of *DEF* activity (Figure 1G) and strengthens the importance of a continuous *DEF* function until late stages of petal development to suppress photosynthesis. Other identified genes were more diverse in their functions, including enzymes like β-glucosidases, catalases, and acyl-CoA oxidases or giberellin-induced proteins and plasma membrane intrinsic proteins.

Expression Analysis of Selected Target Genes Corroborates Dependency on the *DEF* Function

Twenty-one genes were selected as representatives for different regulated processes to confirm by RT-PCR studies their dependence on the *DEF* function. For 19 out of 21 selected genes, expression differences detected after abolishing *DEF* activity for 24 and 72 h correlated with the differences detected using array experiments (nine are shown in Figure 6A in an extended analysis, 12 are shown in supplemental data online). Thus the M-CHiPS analysis (Fellenberg et al., 2002) for array data processing and quality control is a reliable method to detect genes that are regulated by *DEF* with changes down to 1.2-fold. This value applies to genes expressed above an intensity threshold that disregards 80% of the spotted genes as not being transcribed under the applied experimental conditions. Out of the 19 target genes, nine were selected that responded strongly and rapidly toward a reduced *DEF* function, including *DEF* itself. To further test the directness of their regulation by *DEF*, *def*-101 flowers were shifted for shorter time spans (0, 4, 8, 12, 24, and 72 h) from the permissive to the nonpermissive temperature at stage 3, and petals were processed for semiquantitative RT-PCR experiments (Figure 6A). Normalization was performed using Ran3 (EST 018_6_06_k11), a small GTPase identified in macroarray experiments as an invariantly expressed gene. Furthermore, RT-PCR experiments with floral and vegetative wild-type organs were conducted to investigate the overall expression pattern of the selected genes (Figure 6B). *DEF* expression drops already after 4 h of heat treatment and decreases thereafter continuously (Figure 6A). This confirms rapid degradation of DEF proteins upon a short temperature increase and reflects a disturbed autoregulatory expression control (Zachgo et al., 1995). However, some residual expression still remains and appears to be independent of the autoregulatory control. GDSL-lipase expression is no longer detectable after 72 h, reaching the lowest RT-PCR expression value of all investigated genes. LTP expression decreases after 12 h of *DEF* reduction. LTP and GDSL-lipase are both strongly expressed in petals and slightly weaker in stamens, and the latter one reveals also a weak carpel expression. Their expression patterns overlap with the *DEF* expression, which is confined to petals and stamens and is also weakly detectable in carpels (Figure 6B), supporting the regulatory function of *DEF*. Interestingly, expression dynamics of α- and β-tubulins are similar, suggesting coregulation to allow heterodimer formation and thereby microtubule assembly. Expression of a calmodulin-like gene, a putative calcium sensor, and an extensin-like protein, representing cell wall related processes, decreases gradually upon abolishing the *DEF* function for extended time spans (Figure 6A). Slight fluctuations in the 4, 8, or 12 h expression levels might be caused by expression differences as a result of a circadian control because harvesting at identical time points was not feasible for these short time spans. Expression of these genes is strongest in petals and stamens but also detectable at reduced levels in sepals and carpels, as well as in vegetative organs (Figure 6B). *DEF* might thus control expression of these genes, but their broad expression range indicates that other factors regulate their expression outside of the petal/stamen context.

The repressed target genes β-glucosidase and Rubisco activase show enhanced expression levels upon *DEF* reduction, the latter one revealing a delayed response (Figure 6A). Absence of expression in petals and stamens is supportive for a direct negative regulatory function of *DEF*. Both genes are weakly expressed in *def*-101 petals at stage 3 at the permissive temperature (Figure 6A), likely because of the slightly reduced *DEF* function in the *def*-101 mutant compared with wild-type flowers (Zachgo et al., 1995). Thus, at 15°C, the *DEF* activity level seems to be already below the threshold required for their full repression in petals of the *def*-101 mutant. In wild-type carpels, quantitative requirements for the *DEF* function to suppress Rubisco activase might be low, and weak *DEF* expression suffices to repress its expression in the fourth whorl (Figure 6B).

In summary, RT-PCR analyses demonstrate that expression of the selected genes was sensitive to shortened time spans of an altered *DEF* function. Therefore, these genes represent target genes whose transcription might be directly controlled by *DEF*.

Analysis of Tissue-Specific Expression of Target Genes

Tissue-specific expression of the selected early target genes was determined by in situ hybridizations on serial cross sections through the bottom and upper part of stage 3 wild-type flowers (Figure 7A). In the basal flower part, *DEF* is expressed almost uniformly throughout the lower tube formed by five fused petals and in the four stamen filaments (Figure 7B). Expression is stronger in epidermal cell layers than in internal tissues. In agreement with RT-PCR analyses of expression in individual organs, *DEF* is also expressed in carpels, mainly in valves and ovules. A similar pattern was observed in the upper part of the flower, formed by the upper and lower lobes. However, *DEF* expression is enhanced in the extensively folded edges of the dorsal petals (Figure 7C).

Analysis of six activated target genes revealed that transcription of the LTP, GDSL-lipase, and the extensin-like genes is restricted to distinct tissues within the second and third whorl organs (Figures 7D to 7I), whereas the α- and β-tubulin and calmodulin-like genes are more uniformly expressed throughout

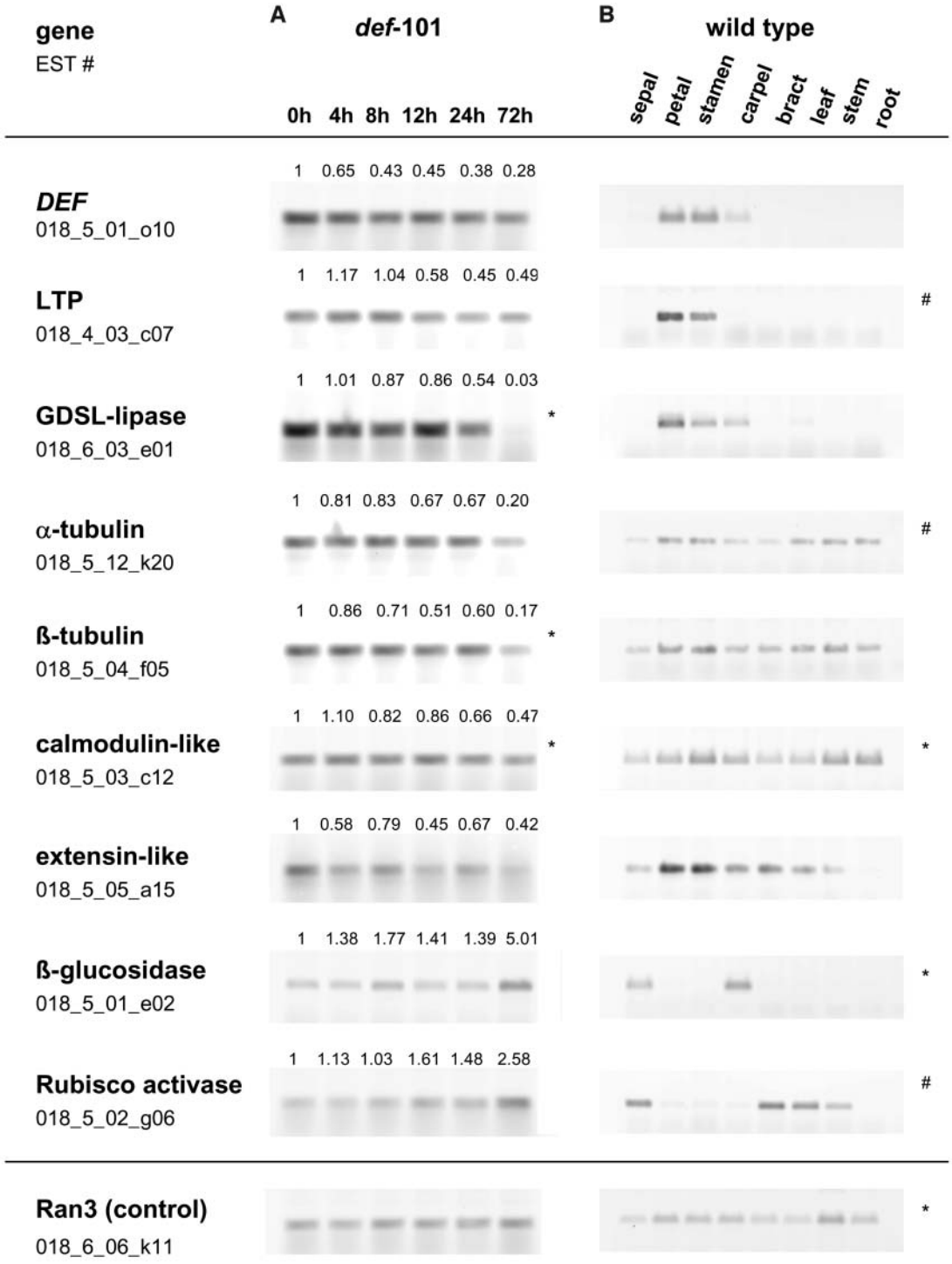

Figure 6. RT-PCR Expression Studies of Selected Target Genes.

Six activated, two repressed target genes, and *DEF* were analyzed by RT-PCR experiments. EST clone identifiers are specified. PCRs were conducted with 22 cycles. Labeling with (*) and (#) indicates that 25 and 20 cycles were conducted, respectively.

(A) First strand synthesis was prepared from total RNA extracted from *def*-101 petals cultivated at the permissive temperature (15°C) until stage 3 and then shifted for 0, 4, 8, 12, 24, and 72 h to the nonpermissive temperature (26°C). The small GTPase Ran3 was used as a control that was identified in macroarray experiments as being indifferently expressed under these conditions. Values given above the gel pictures are the ratio of the signal in shifted *def*-101 petals to nonshifted *def*-101 petals, normalized relative to the Ran3 signal.

(B) Organ-specific expression of selected *DEF* target genes. To determine the organ-specific expression of target genes, total RNA was isolated from sepals, petals, stamens, and carpels of wild-type Antirrhinum flowers at stage 3 and from bracts, leaves, stems, and roots. RT-PCRs were conduced with the indicated cycle numbers. As a control, expression of Ran3 was analyzed.

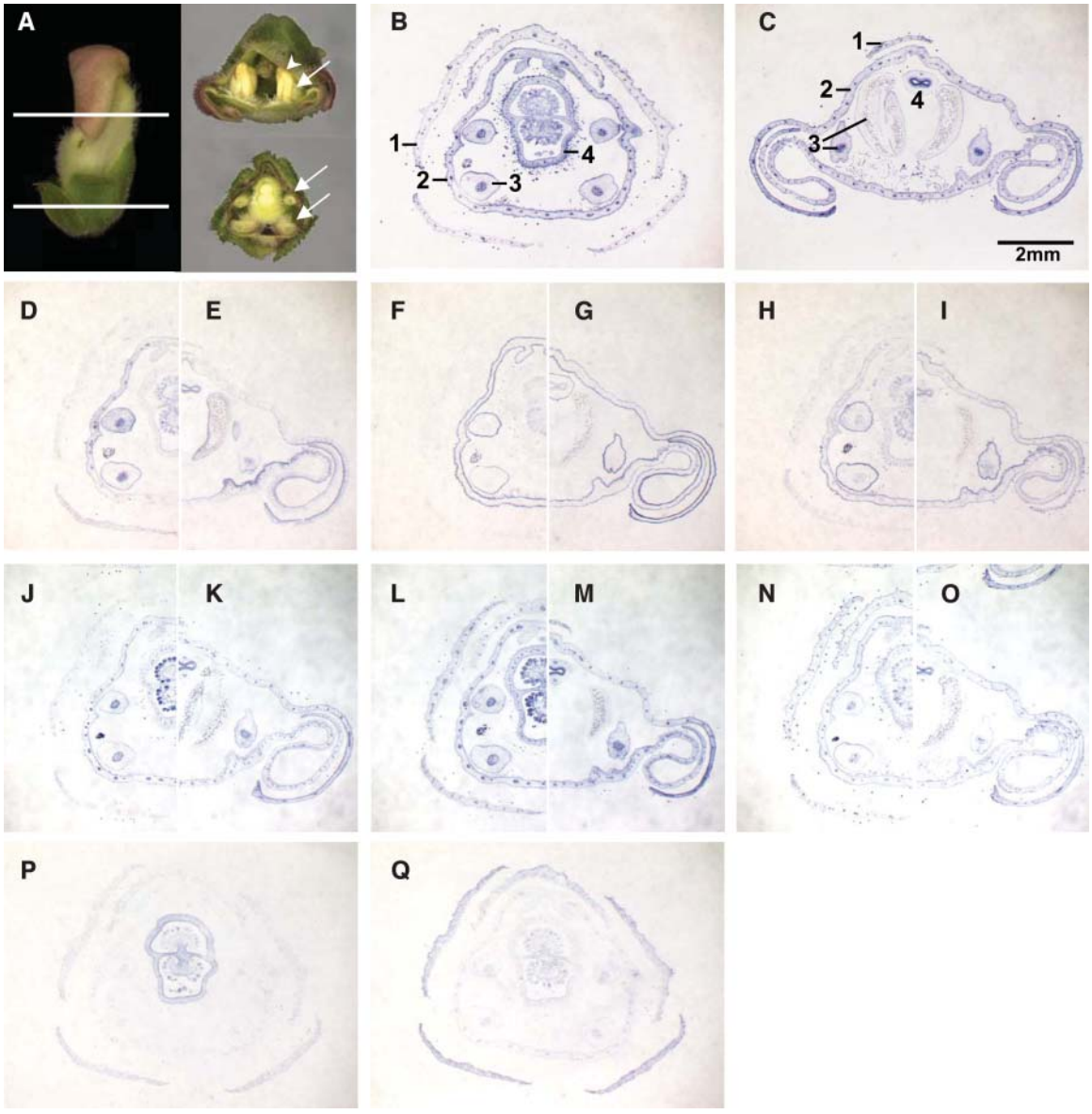

Figure 7. In Situ Analysis of Selected *DEF* Target Genes in Wild-Type Flowers.

Serial sections through upper and bottom parts of wild-type flowers at stage 3 were made and combined on one slide to guarantee identical hybridization conditions. Bar is shown representatively for all in situ sections in **(C)**.

(A) For orientation, cutting planes are shown along with the corresponding transverse sections. Cut filaments are indicated by arrows, one anther is marked by an arrowhead.

(B) and **(C)** *DEF* staining of transverse sections made through the bottom and upper part of a wild-type stage 3 flower, respectively. *DEF* is expressed throughout petals in upper and lower lobes. Staining was detected in filaments, including vasculature, and in the fourth whorl. Microsporogenous tissue and sepals are largely devoid of signal; weak expression can be detected in sepal vasculature. Numbers 1, 2, 3, and 4 designate the four floral whorls.

(D) and **(E)** LTP expression is confined to petals and stamens. Expression is stronger in adaxial epidermis of highly folded dorsal and lateral petals **(E)**.

(F) and **(G)** GDSL-lipase is strongly expressed in the abaxial and adaxial epidermal cell layers of petals and stamens and at attenuated levels in ovules and epidermal cells of the style.

(H) and **(I)** The extensin-like gene is predominantly expressed in petals and stamens, where expression is stronger in epidermal cell layers. Weak signal was detected in fourth whorl ovules.

(J) and **(K)** mRNA of α-tubulin is localized in petals and stamens as well as in ovules.

(L) and **(M)** β-Tubulin expression overlapping with α-tubulin expression and expanding further into valves and sepals.

(N) and **(O)** Calmodulin-like gene expression is detected throughout the whole flower and slightly increased in folded petal areas.

(P) β-Glucosidase is weakly expressed in sepals and stronger in carpels.

(Q) Rubisco activase is predominatly expressed in sepals.

these organs (Figures 7J to 7O). LTP is strongly expressed in the epidermal cell layer of the dorsal and lateral petal edges that, upon maturation, will be unfolded and exposed to pollinators (Figure 7E). GSDL-lipase expression was exclusively detected in the inner and outer epidermis of petals and filaments (Figures 7F and 7G). A similar expression pattern was detected for the extensin-like gene, however, with an additional weak staining throughout the two whorls. In addition, weak expression in ovules was observed, confirming the RT-PCR analysis (Figures 7H and 7I). These observations emphasize the importance of the epidermal petal cell layers that function not only in scent and sheen production but also make a major contribution to the overall petal shape (Noda et al., 1994; Perbal et al., 1996; Dudareva et al., 2000; Efremova et al., 2001). For the α- and β-tubulins, overlapping expression was detected in petals and stamens (Figures 7J to 7M). Stronger labeling of the dorsal petal edges might indicate an increased requirement of microtubules during the rapid expansion phase of these structures. The calmodulin-like gene, likely involved in cell signaling, is transcribed in all whorls, with a weakly enhanced expression in the folded edges of the petals (Figures 7N and 7O). Supporting the organ-specific RT-PCR experiments, the repressed target genes β-glucosidase and Rubisco are expressed in sepals, and β-glucosidase expression was also detected in carpels (Figures 7P and 7Q).

Furthermore, in situ studies were conducted on sections from *def*-101 flowers at stage 3, shifted for 0, 24, and 72 h from the permissive to the nonpermissive temperature (Figure 8). Thereby, tissue-specific expression pattern changes were monitored during the time course of reducing the *DEF* function. Representative data are shown for one activated and one repressed target gene. Expression of the activated target gene GSDL-lipase gradually decreases in petal and filament epidermal cell layers until no signal is any longer detectable after abolishing *DEF* activity for 72 h (Figures 8A to 8C). Expression in carpels is not affected. Conversely, expression of the repressed target gene Rubisco activase is enhanced in second whorl organs during prolonged shift periods of reduced *DEF* activity (Figures 8D to 8F). Increased expression is more pronounced in ventral petals (Figure 8F), which is in accordance with our morphological data showing more severe effects on the ventral part of the flower (Figure 1G).

In summary, in situ experiments defined tissue-specific differences in expression patterns of the selected *DEF* target genes and confirm macroarray and RT-PCR data.

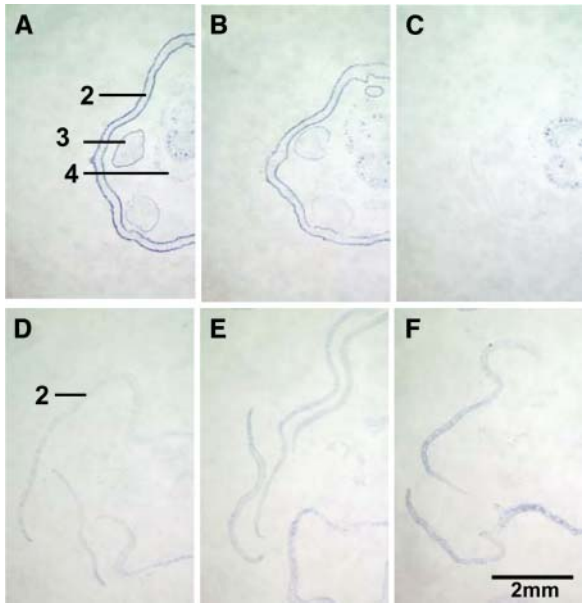

Figure 8. Effect of a Decreased *DEF* Function on GDSL-Lipase and Rubisco Activase Expression Patterns.

Serial sections were made from *def*-101 flowers at stage 3, shifted for 0 (**[A]** and **[D]**), 24 (**[B]** and **[E]**) and 72 (**[C]** and **[F]**) h from the permissive to the nonpermissive temperature. Sections were combined on one slide to compare expression levels. Numbers 2, 3, and 4 designate the second, third, and fourth whorl. Bar is shown representatively for all sections in **(F)**.

(A) to **(C)** GDSL-lipase expression at the bottom of the flower gradually vanishes from the epidermal cell layers of petals and stamens during prolonged time spans of reduced *DEF* function. After 72 h, no mRNA expression can be detected. Bottom sections demonstrate that expression in ovules is not affected by reducing the *DEF* function. Sepals were devoid of signal (data not shown).

(D) to **(F)** Expression of Rubisco activase is already weakly detectable in upper parts of *def*-101 petals, cultivated at the permissive temperature. Upon a reduction of the *DEF* function, expression increases steadily in the second whorl, being more pronounced in the ventral petal. Anthers and style are not stained and thus are not visible.

DISCUSSION

In an effort to gain deeper insights into petal morphogenesis, a broad survey of petal development was performed by comparing late petal and sepal development at defined stages. Given the known homeotic control of petal development by the *DEF* gene, these studies identified genes that are directly or indirectly regulated by this MADS box transcription factor. Subsequently, a profiling analysis was employed exploiting the conditional *def*-101 mutant for identification of putative direct *DEF* petal target genes. These studies took advantage of the large size of the Antirrhinum flower for expression profiling studies with distinct floral organs.

Late Stages of Petal Development Reveal Highly Dynamic Transcriptome Changes

High-throughput analysis using macroarrays comprising >11,600 Antirrhinum unigenes was conducted to compare petal and sepal expression profiles. Regulation of functional categories was investigated throughout four petal developmental stages starting at a floral bud size of 0.5 cm until a 4.0-cm-long mature flower was formed 11 d later. As a reference, a mixture of sepals was used. The M-CHiPS method applied for array data analysis has been already shown for other data to be suitable for studying subtle transcriptional changes (Lagorce et al., 2003). More than 90% (19/21) of genes identified by expression profiling

as being differentially expressed with changes down to 1.2-fold (applying intensity thresholds excluding 80% of the spotted genes as not expressed) were verified by independent expression studies.

In total, 537 ESTs were found to be differentially expressed in at least one investigated stage, dividing into 322 activated and 226 repressed ESTs, and comprising 11 ESTs assigning into both groups. Considering that these data include approximately one-fifth redundant ESTs as ~22% of the unigenes were spotted twice on the arrays and that the ESTs represent only ~40% of the total cDNAs, the total number of upregulated genes during late petal stages might be in the order of 600 or more. Using whole flowers from different stages of Arabidopsis mutants and also transgenic inflorescences, 200 (Zik and Irish, 2003) and >1100 genes, including ~600 pollen-specific ones (Wellmer et al., 2004), were predicted as being regulated in petals and/or stamens by the Arabidopsis class B genes *AP3* and *PI*. Identification of the significantly larger number of differentially expressed Antirrhinum genes most likely results from using mRNA from distinct organs and stages, which minimizes blurring of transcript differences and thus increases the sensitivity for detection of expression differences. The estimated number of 600 genes represents genes whose expression is differentially regulated between sepals and petals, but they also include genes that are expressed in stamens and carpels, as it was shown for some of the selected *DEF* target genes (Figure 6B). It will be intriguing to determine by floral organ comparisons a group of exclusively petal-specific genes with this system in the future.

The number of genes that are upregulated during petal development increases steadily from stage 2 on. As organ harvesting for the sepal/petal comparison started in stage 1, the identified 104 upregulated ESTs likely record an accumulating effect of expression differences from earlier petal stages. The functional category cell cycle and DNA processing is highly overrepresented during stage 1, as reflected by increased expression of DNA replication markers, as for instance, histone H4. The level of these transcripts drops to an average level at stage 2; thus, Antirrhinum petal growth is realized mainly by cell division processes until flowers reach a size of 0.8 cm. After stage 2, the number of activated genes continuously increases mainly by strong upregulation of stage-specifically expressed ESTs. In total, 2851 genes showed an expression level high enough in at least one stage to be considered for petal profiling analysis. Thirty-three and 114 of the analyzed ESTs were specifically upregulated in stages 3 and 4, respectively. The highly dynamic transcriptome changes reflect the need for specialized proteins to participate in the final maturation phase of petal development. Analysis of 20 selected functional categories showed that especially genes with a metabolism-related function are strongly upregulated. Similar results were obtained by functional classification of 2100 rose petal genes (Guterman et al., 2002). Closer inspection of functions by individual BLAST analyses showed that during stages 3 and 4 genes involved in processes associated with cell growth are upregulated. Enzymes, such as pectinacetylesterases, modifying cell wall components, or structural cell wall proteins, like extensins, were identified. The observed upregulation of aquaporins, water channel proteins, and tonoplast proteins reflects an alteration of turgor pressure driving cell expansion during the final petal growth phase (Schäffner, 1998). Clearly, there is a requirement for primary metabolites as well as for secondary metabolites to allow final petal growth. Genes involved in secondary metabolite production with specialized function in the epidermal cell layer were identified as being upregulated. For instance, *S*-adenosyl-L-methionine:benzoic acid carboxyl methyltransferase is the final enzyme in the biosynthesis of the scent compound methyl benzoate (Dudareva et al., 2000), anthocyanidin synthase catalyzes the penultimate step in the biosynthesis of the anthocyanin class of flavonoids (Wilmouth et al., 2002), and *CER1* is involved in wax biosynthesis (Aarts et al., 1995).

Surprisingly, the proportion of unclassified proteins was higher in the petal expressed transcripts compared with their general representation in the Antirrhinum EST collection. This group might contain genes with specialized functions in secondary metabolite production because they are highly divergent among plant genomes and therefore might escape from identification by sequence comparison (Pichersky and Gang, 2000).

Altogether, 156 to 180 ESTs were repressed during the four petal stages compared with sepals. In contrast with the upregulated ESTs, only a low number, 34 ESTs, were stage-specifically repressed. The majority of the repressed ESTs exerts a function associated with photosynthesis, in accordance with plastid ontogeny in Arabidopsis, where green chloroplasts are initially formed in all young floral organs. During further petal differentiation, chlorophyll content decreases and redifferentiation to leucoplasts occurs while chloroplasts remain only at the base of petals (Pyke and Page, 1998).

Expression of More Than 100 Genes Is Affected by a Reduced *DEF* Function at Petal Stage 3

Petal stage 3 was chosen to identify target genes, likely to be under direct control of *DEF.* This stage is characterized by the onset of rapid petal growth realized mainly by cell elongation processes, and we showed that novel, stage-specific transcripts start to accumulate. Expression changes were investigated with the *def*-101 mutant after reducing the *DEF* function for 24 and 72 h by increasing growth temperature. After subtracting generally temperature-sensitive genes detected in control experiments, 101 unigenes were identified that show a significantly altered expression level in at least one condition (see supplemental data online). Sixty-seven of these target genes were also detected in the sepal/petal comparison, indicating a high overlap of the identified genes in the two different experiments but reflecting also differences in culturing conditions and different *DEF* expression levels between *def*-101 and wild-type flowers. Expression of 46 genes was affected by reduction of the *DEF* function for 24 h. The expression of these 27 repressed and 19 activated target genes could be directly controlled by *DEF*. Prolongation of the reduction period for up to 72 h increased the number of affected genes to 93, with almost equal numbers of activated and repressed genes. Thus, for normal petal development to proceed, the expression of similarly sized groups of genes has to be activated and repressed by *DEF*. Furthermore, the importance of

DEF to act constantly as a repressor of sepal-specific genes during late petal development corroborates our morphological data.

Assuming that the EST collection represents ~40% of the total Antirrhinum unigene set, we estimate that >200 target genes might be regulated by *DEF* at stage 3. As we have shown, highly dynamic transcriptome changes occur during the four late petal developmental stages. Therefore, this number is representing only a subset of the total *DEF* petal target genes.

Putative Direct *DEF* Target Genes Are Involved in Different Processes Associated with Cell Growth during Late Petal Development

Functional categorization of *DEF* target genes showed that mainly genes belonging to the groups metabolism, transport facilitation, energy, and control of cellular organization were strongly overrepresented. For detailed analysis, target genes were selected that are representative for different processes cooperating during petal development. Eight genes that showed a strong expression level change after the *DEF* function was abolished for 24 h were further analyzed by RT-PCR studies where *DEF* activity was reduced for shorter time spans (4, 8, and 12 h). For all selected genes, changes in expression levels were detected during the shortened time spans. Four of them responded already after 4 h and two after 8 and 12 h of *DEF* reduction, respectively. Toward the goal to investigate if quickly responding genes represent direct *DEF* target genes, we have started to analyze their promoters. Preliminary data show that they contain CArG-box motifs (data not shown). Interestingly, the extensin-like promoter contains two nearby CArG-boxes that could be required, similarly to the two CArG-box motifs in the *GLO* promoter, for binding a DEF ternary protein complex (Egea-Cortines et al., 1999).

Expression analysis data, together with putative gene functions, are discussed separately for the different target genes.

DEF Regulates a Group of LTPs

Four LTPs were isolated as being regulated by the *DEF* activity, three as activated, and one as a repressed target gene. We investigated the expression of the activated LTP 018_4_03_c07 that was also found to be strongly upregulated (>12-fold) in the sepal/petal comparison in more detail. Its expression level decreases after reducing the *DEF* function for 12 h. At stage 3, it is exclusively expressed in petals and stamens, thus representing an interesting candidate for a direct target gene of *DEF*. Cell-type specific investigation by in situ analysis revealed that this LTP is expressed in restricted areas in petals. A signal was localized in the upper dorsal petals, predominately in parts that, upon unfolding, will be exposed to pollinators. LTPs can mediate the transfer of phospholipids between membranes in vitro (Zachowski et al., 1998). However, an Arabidopsis LTP was localized in the cell wall, questioning their function in catalyzing intracellular lipid transfer between membranes (Thoma et al., 1993). Other plant LTPs have been shown to be expressed in a large variety of different floral tissues, indicating that they are involved in various processes (Kotilainen et al., 1994; Rubinelli et al., 1998). The identification of Antirrhinum LTPs as *DEF* target genes suggests a function during late petal and stamen development.

GDSL-Lipases

A GDSL-lipase revealed the strongest expression response of all investigated target genes and was no longer detectable by in situ and RT-PCR experiments after 72 h of *DEF* reduction. Its expression is strongest in petals and slightly weaker in stamens. Similar to *DEF*, very weak expression was also detected in carpels. In situ analysis shows that the expression of this Antirrhinum GDSL-lipase is restricted to the epidermal cell layers of petals and stamens. The GDSL-lipase might thus function during differentiation of the highly specialized epidermal cells. GDSL-lipases are lipolytic enzymes with an active site, the name-giving conserved GDSL amino acid sequence (Upton and Buckley, 1995). Regulation of GDSL-lipases genes might be conserved between Scrophulariaceae and Brassicaceae class B genes, as two independent studies identified a GDSL-lipase from Arabidopsis as a gene that is not expressed in mutants lacking petals (Zik and Irish, 2003; Wellmer et al., 2004).

Structural Proteins Involved in Cell Morphogenesis

Expression of α- and β-tubulins responded similarly to an altered *DEF* function. Both genes are expressed ubiquitously throughout the plant, with the highest expression level in petals and stamens. The final cell shape is determined by extent and direction of cell expansion, requiring regulated deposition of cellulose microfibrils in the innermost cell wall. It has been suggested that the orientation of cortical microtubules, mainly composed of α- and β-tubulins forming heterodimers, determines cell wall deposition in elongating cells (Mayer and Jürgens, 2002). The Antirrhinum α-tubulin reveals >95% amino acid sequence identity to the Arabidopsis α-tubulin 6, 4, and 2 proteins (Kopczak et al., 1992). The double mutant *lefty1 lefty2* of the α-tubulin 6 and α-tubulin 4 genes produces defective microtubules, causing severe abnormalities during hypocotyl, root, and flower morphogenesis (Abe et al., 2004). Mutant flowers produce shorter anther filaments as directional cell growth is impaired and form twisted petals. Our data indicate that *DEF* coordinates upregulation of α- and β-tubulin expression during the rapid cell elongation phase in Antirrhinum petal and stamen development. In situ analysis showed overlapping expression patterns in stamens and petals with a higher expression level within the dorsal petal edges. Coregulation of α- and β-tubulin expression provides a means to form microtubular structures required for the final growth phase of the petal. Interestingly, the serum response factor, an animal MADS box transcription factor essential for mesoderm formation in mouse embryos, also regulates cytoskeletal proteins, particularly the expression of different actins (Schratt et al., 2002).

Various Genes Participate in Cell Wall Formation

As mentioned above, the cell wall affects cell shape and function. We identified several structural proteins and enzymes participating in cell wall formation as *DEF* target genes, including pectin modifying enzymes, cell wall proteins, and extensin-like genes that were strongly upregulated during later petal development stages. An extensin-like gene was investigated in more detail, revealing a rapidly decreased expression upon reducing the *DEF* function. Extensins belong to the HRGP superfamiliy, a major class of structural proteins in the primary cell wall of higher plants (Kieliszewski and Lamport, 1994; Cassab, 1998). Extensins share the massive presence of Pro residues occurring in repetitions of at least two consecutive Pro. These abundant proteins represent the major cell wall scaffolding components together with other HRGP subgroups, such as repetitive Pro-rich proteins, arabinogalactan-proteins, and lectins. An extensin-like gene from tomato (*Lycopersicon esculentum*) is expressed in the root hair differentiation zone and is involved in oriented cell elongation leading to cellular tip growth of tomato root hair (Bucher et al., 2002). Two *LEUCINE-RICH REPEAT EXTENSIN* genes (*LRX1* and *LRX2*) were recently cloned from Arabidopsis and shown to be required for cell morphogenesis of root hairs (Baumberger et al., 2001, 2003). The intracellular cytoskeleton provides the means by which vesicles are translocated to the cell wall to deliver components required for cell elongation. Coregulation of these processes by one key transcription factor, such as *DEF*, provides an effective mechanism to control this interdependency.

Cell Signaling

Calcium signaling orchestrates responses to cellular stimuli. Intriguingly, a calmodulin-like gene was identified as a target gene that is ubiquitously expressed with higher expression levels in petals, stamens, carpels, stems, and roots. Calmodulin serves as a universal calcium sensor in all eukaryotes, mediating calcium action by regulating the function of many targets in diverse cellular pathways (Zielinski, 1998). The requirement of cell-signaling processes for petal organogenesis has been demonstrated by the observation that *DEF* acts non-cell-autonomously and by quantitative growth modeling, predicting a long-range signal to control petal growth direction (Perbal et al., 1996; Rolland-Lagan et al., 2003).

Repressed *DEF* Target Genes Comprise a Large Group of Genes Associated with Photosynthesis

Homology comparison showed that a large group of genes whose expression is repressed by *DEF* exerts functions related to photosynthesis. Genes like Rubisco small chain, Rubisco activase, and photosystem II protein precursor were found to be highly expressed in sepals and upregulated upon a reduction of the *DEF* function for 24 h. As a representative of this group, we analyzed Rubisco activase in more detail. The enzyme is expressed in sepals, bracts, leafs, and stems. It activates Rubisco, the key enzyme of photosynthesis, by a carbamylation reaction (Werneke et al., 1989). As indicated by comparative petal expression profiling, Rubisco activase is repressed continuously throughout petal development, and we showed that its expression level is increased after 12 h of *DEF* reduction. Together with the morphologically visible petal to sepal transformations, this demonstrates the rapid and long maintained potential of the second whorl organs to adopt a sepaloid structure. Although chloroplasts redifferentiate during petal development into leucoplasts (Pyke and Page, 1998), they seem to keep the plasticity that allows them to quickly convert into photosynthetically active plastids even at late stages of petal development.

Various other enzymes, involved in different metabolic processes, were identified as repressed genes. Detailed expression studies were conducted with a β-glucosidase, an enzyme hydrolyzing conjugated β-glucoside compounds present in plant secondary metabolism. Physiological functions of β-glucosidases are broad as they depend on the function of the molecule released after hydrolysis. Plant development and growth can be affected by regulating cell division via release of active phytohormones from their respective inactive glycoconjugated forms (Brzobohaty et al., 1993). The enzymes participate in the modification of oligosaccharides in cell walls (Akiyama et al., 1998) and play a role in defense metabolism against pathogens (Sue et al., 2000) and in the production of secondary metabolites such as flavonoids and lignins (Leinhos et al., 1994). Interestingly, β-glucosidase expression is confined to sepals and carpels only, as expected from a target gene negatively regulated by *DEF*.

Tissue-Specific Target Gene Expression Indicates Suborgan Specific Regulation of Gene Expression

In situ studies showed that expression of the two putative direct target genes, LTP and GDSL-lipase, is restricted to distinct tissues within petals, in particular to epidermal cell layers. These genes represent good candidates for being directly and exclusively controlled by *DEF* because their expression patterns overlap with *DEF* expression domains. A wild-type petal comprises about six cell layers. However, only the epidermal cell layer has been reported to exert specialized functions, such as scent compound production and formation of characteristic conical cells contributing to the velvet sheen of Antirrhinum petals. The LTP and GDSL-lipase target genes might thus participate in specialized functions of epidermal cells. Other investigated target genes show a broader expression throughout petals and stamens with a tendency for higher expression at the edges of dorsal petals where rapid expansion and unfolding during the final maturation phase occurs. Because they were also expressed at lower levels in vegetative tissues, their expression seems to be not exclusively controlled by *DEF*.

We detected only one other transcription factor, the MADS box gene *DEFH84*, whose expression is upregulated by *DEF*. From this observation, we conclude that *DEF* seems to exert its regulatory control until late stages rather directly, without delegating transcriptional control functions to a large number of other intermediate transcription factors. Showing that expression of some target genes is confined to various subdomains of *DEF* expression raises the question of how this spatial restricted target gene regulation is achieved. Formation of multimeric complexes has been demonstrated for MADS box proteins and thus

provides a mechanism by which different binding specificities for various target genes can be generated (Egea-Cortines et al., 1999; Honma and Goto, 2001; Ferrario et al., 2003). In the future, advancement of proteomics technologies will allow in vivo analysis of MADS box protein complex composition and help to unravel different interactions in the control of distinct target genes.

Former studies have shown a high degree of conservation in target gene regulation throughout the plant kingdom. The Antirrhinum class B gene *DEF* can functionally substitute the orthologous Arabidopsis class B gene *AP3* by complementing the *ap3* mutant phenotype (Samach et al., 1997). Developmental profiling and target gene studies of floral organs from model species besides Arabidopsis allow conducting comparative studies. Thereby, the question can be addressed to which extent spatial and temporal expression alteration and/or recruitment of novel target gene functions contributed downstream of the key regulatory genes to generate the floral organ diversity observed today.

METHODS

Plant Growth, Harvesting, and Experimental Setup

Wild-type plants (line 165E) and *def*-101 mutants were cultivated under identical light intensities and day–night regimes as described by Zachgo et al. (1995). After formation of two internodes, *def*-101 and control wild-type plants were transferred to climate chambers and grown at either 15°C (permissive temperature) or 26°C (nonpermissive temperature). Plants with flowers in appropriate developmental stages were shifted in parallel at the same 24, 48, and 72 h time points, except for the 4, 8, and 12 h shifts, for which time points had to be adapted.

Macroarrays were hybridized with three technical replicate probes per condition. Plant material originated from two biological samples of different nature, each prepared from at least eight pooled plants.

ESTs and Macroarray Setup

For construction of the EST library, double-stranded cDNA was prepared according to the Clontech SMART protocol (Palo Alto, CA) from a mixture of RNAs derived from 12 different vegetative and reproductive organs from defined developmental stages. Normalization was achieved by denaturing and reannealing the PCR products followed by separation of single-stranded and double-stranded molecules on a hydroxylapatite column (Bonaldo et al., 1996). The unigene set, comprising 11,615 genes, was determined by random sequencing of >25,000 ESTs, cloned into the pBS KS+ vector (Stratagene, La Jolla, CA). Macroarrays were produced (Eurogentec, Seraing, Belgium) by spotting 14,186 partially from their 5′ end (MWG, Ebersberg, Germany) sequenced *Antirrhinum majus* ESTs in a double offset pattern (4 × 4) on 22 × 22-cm nylon membranes. The 14,186 ESTs include ~22% redundant genes that were spotted twice on the filters.

Assembly and clustering of the ESTs using the CAP3 contig assembly program (Liang et al., 2000) allowed us to determine unigenes with an average sequence length of ~600 bp.

RNA Preparation and Labeling

Total RNA was extracted using the RNeasy plant mini kit (Qiagen, Hilden, Germany), and concentration was determined via OD measurement.

For probe preparation, 25 μg of total RNA were mixed with 0.5 μg of oligo(dT)$_{15}$ (Invitrogen, Karlsruhe, Germany) and diethylpyrocarbonate-treated water up to a volume of 11 μL. The sample was heated to 70°C for 10 min and subsequently cooled to 43°C. First strand synthesis was performed in a total volume of 30 μL using 200 units of Superscript II reverse transcriptase (Invitrogen) in the presence of 1× Superscript II reverse transcriptase buffer (Invitrogen), 0.01 M DTT (Invitrogen), 1 mM each dATP, dGTP, and dTTP, 5 μM dCTP, and 30 μCi of [α-^{33}P]dCTP. After 60 min at 43°C, an alkaline hydrolysis of the RNA was conducted by adding 1 μL of 1% SDS, 1 μL of 0.5 M EDTA, and 3 μL of 3 M NaOH, and the mixture was incubated for 30 min at 65°C and subsequently for 15 min at room temperature. The solution was then neutralized with 10 μL of 1 M Tris-HCl, pH 8.0, and 3 μL of 2 M HCl. After the addition of 5 μL of 3 M sodium acetate, pH 5.3, 5 μL of tRNA (10 mg/mL) and 60 μL of isopropyl alcohol the cDNA was precipitated at −20°C for 30 min, pelleted by centrifugation, and resuspended in 100 μL of deionized water. Incorporation of ^{33}P into the first strand cDNA was checked by scintillation counting. For consistent results, only probes with an incorporation level >30% of the initial input radioactivity were used for hybridization.

Macroarray Hybridization

Before the first hybridization, a mock treatment was conducted with all EST filters, comprising a complete round of prehybridization, hybridization, and stripping without adding a radioactively labeled probe. Macroarrays were prehybridized for 1 h in 25 mL of 7% SDS, 0.5 M sodium phosphate, pH 7.2, and 1 mM EDTA at 65°C. For hybridization, cDNA probes were denatured for 5 min at 100°C and added directly to the prewarmed solution. Hybridization was performed for 16 h at 65°C. Filters were briefly rinsed in a solution containing 40 mM sodium phosphate, pH 7.2, and 0.1% SDS, followed by two 30-min washes in 40 mL of the same buffer at 65°C. Macroarrays were exposed to phosphor screens (Amersham Biosciences, Freiburg, Germany) for 21 h. Signal detection was performed by a PhosphorImager (Typhoon 8600; Amersham Biosciences). For stripping, filters were shaken in a boiled solution of 5 mM sodium phosphate, pH 7.2, and 0.1% SDS until temperature cooled down to room temperature. This procedure was repeated before reusing the filter until signal strength decreased >90%.

Data Analysis

Spot intensities were quantified using the A.I.S. Array Vision version 5.0 software (Imaging Research, St. Catharines, Ontario, Canada). Normalization and filtering of raw data was conducted with the M-CHiPS (Fellenberg et al., 2002), a MATLAB-based tool meeting the M.I.A.M.E. criteria (Brazma et al., 2001). After subtraction of the local background, normalization was performed according to Beissbarth et al. (2000) and Fellenberg et al. (2001). Each hybridization experiment was normalized with respect to the gene-wise median of the control condition (sepals or not shifted *def*-101 petals at stage 3) that was referred to as a standard. Normalization factors were computed on the basis of the majority of spots, as transcription levels of the majority of genes were unaltered under investigated conditions. For six spot replicates (duplicates from three independent hybridizations) of every condition, a gene-wise intensity median was calculated (Fellenberg et al., 2001). The whole data set, comprising the experiment annotations, and the complete lists of raw, fitted, and statistically processed data of the single hybridizations as well as the averaged conditions are deposited at http://m-chips.org/antirrhinum_petal_development.

Data quality was reviewed by calculating the Pearson correlation coefficients for spot replicates of the same filter or different hybridizations, respectively (Draghici, 2003). Correlation coefficients for two hybridizations investigated within the same condition were always above

0.8, ensuring low technical variance between the compared samples and thus a good reproducibility (see supplemental data online). An intensity threshold was applied to avoid false positives showing high ratios but very low absolute intensity signals. The genes that have been spotted on our array have not been specifically selected for being transcribed under the studied conditions. In accordance with previous studies processing large data sets, we considered within every condition ~80% of the genes showing signal intensities near background levels to be not transcribed (Beissbarth et al., 2000) and excluded them by intensity threshold. Genes not transcribed under any of the investigated conditions were not considered for further studies. Significance levels were checked by two stringency criteria, and genes considered to be differentially expressed had to conform at least to the less stringent standard deviation separation (Beissbarth et al., 2000). Data lists of regulated genes with signal intensity ratios are available in the supplemental data online.

Independent RT-PCR analysis were conducted (see supplemental data online) and proved that—after removing 80% of the genes for showing too small intensities—changes down to 1.2 result in a list of target genes with verifiably variant transcription.

Hierarchical cluster analyses were performed using the program GENESIS version 1.2.2 that is based on algorithms from CLUSTER and TREEVIEW developed by Eisen et al. (1998).

For functional analysis, Antirrhinum EST sequences were compared with the *Arabidopsis thaliana* unigene set from NCBI (www.ncbi.nlm.nih.gov/UniGene) using the TBLASTX algorithm. Homologs with an expect value (E-value) of $<2.0\ E^{-12}$ were grouped into 20 selected role categories according to MIPS (http://mips.gsf.de). Clustering of one gene into multiple categories was possible. Sequences that did not reveal an Arabidopsis homolog under these conditions were compiled into the category X (homolog not found).

Expression Studies

Semiquantitative RT-PCR

First strand cDNA was synthesized from 2 μg of total RNA using 200 units of SuperScript II reverse transcriptase (Invitrogen) according to the supplier's instructions. One microliter of cDNA was used as template for a 25-μL PCR reaction with gene-specific primers (see supplemental data online). The PCR reaction was set up as follows: 94°C for 2 min; 20 to 25 cycles of 94°C for 1 min, 56°C for 1 min, 72°C for 1 min, followed by a final extension at 72°C for 3 min. Taq polymerase was purchased from Qiagen, and the PCR mix prepared according to manufacturer's instructions. Seven microliters out of 25-μL reactions were loaded on an ethidium bromide–stained 1.2% (w/v) agarose gel. Quantification of band strength was accomplished as described above by scanning gels with the phosphor imager Typhoon 8600 (Amersham Biosciences) and using Image Quant version 5.1 software (Amersham Biosciences). For normalization of signal strength, Ran3 (018_6_06_k11) was used, shown in macroarray experiments to be invariantly expressed in investigated conditions. Three repetitions were conducted for each gene, and one representative result is shown.

In Situ Hybridization

Digoxigenin-labeled riboprobes of *DEF*, LTP (018_4_03_c07), GDSL-lipase (018_6_03_e01), α-tubulin (018_5_12_k20); β-tubulin (018_5_04_f05), calmodulin-like (018_5_03_c12), extensin-like (018_5_05_a15), β-glucosidase (018_5_01_e02), and Rubisco activase (018_5_02_g06) were made using DIG RNA labeling mix and T3 polymerase from Roche Diagnostics (Indianapolis, IN) according to the manufacturer's instructions. Primers used for PCR template generation containing a T3 polymerase binding sequence are listed in the supplemental data online. *DEF* probe was prepared as described by Perbal et al. (1996). Wild-type and *def*-101 flowers at stage 3 were processed for transverse sectioning and hybridized as described previously by Zachgo (2002).

Sequence data from this article have been deposited with the EMBL/GenBank data libraries under accession numbers AJ558253 to AJ560288, AJ568031 to AJ568983, and AJ786842 to AJ809161.

ACKNOWLEDGMENTS

We thank Anja Hörold for support with the RT-PCR work and Markus Kuckenberg for handling of the EST plasmid stock collection. Sybille Richter and Manfred Pohé are acknowledged for their help in plant cultivation. This work was supported by a grant from the Deutsche Forschungsgemeinschaft to S.Z. (ZA 259/3-1).

Received August 12, 2004; accepted October 1, 2004.

REFERENCES

Aarts, M.G.M., Keijzer, C.J., Stiekema, W.J., and Pereira, A. (1995). Molecular characterization of the CER1 gene of Arabidopsis involved in epicuticular wax biosynthesis and pollen fertility. Plant Cell **7,** 2115–2117.

Abe, T., Thitamadee, S., and Hashimoto, T. (2004). Microtubule defects and cell morphogenesis in the lefty1 lefty2 tubulin mutant of *Arabidopsis thaliana*. Plant Cell Physiol. **45,** 211–220.

Akiyama, T., Kaku, H., and Shibuya, N. (1998). A cell wall-bound [beta]-glucosidase from germinated rice: Purification and properties. Phytochemistry **48,** 49–54.

Baumberger, N., Ringli, C., and Keller, B. (2001). The chimeric leucine-rich repeat/extensin cell wall protein LRX1 is required for root hair morphogenesis in *Arabidopsis thaliana*. Genes Dev. **15,** 1128–1139.

Baumberger, N., Steiner, M., Ryser, U., Keller, B., and Ringli, C. (2003). Synergistic interaction of the two paralogous *Arabidopsis* genes *LRX1* and *LRX2* in cell wall formation during root hair development. Plant J. **35,** 71–81.

Beissbarth, T., Fellenberg, K., Brors, B., Arribas-Prat, R., Boer, J.M., Hauser, N.C., Scheideler, M., Hoheisel, J.D., Schütz, G., Poustka, A., and Vingron, M. (2000). Processing and quality control of DNA array hybridization data. Bioinformatics **16,** 1014–1022.

Ben-Nissan, G., and Weiss, D. (1996). The petunia homologue of tomato gast1: Transcript accumulation coincides with gibberellin-induced corolla cell elongation. Plant Mol. Biol. **32,** 1067–1074.

Bonaldo, M.F., Lennon, G., and Soares, M.B. (1996). Normalization and subtraction: Two approaches to facilitate gene discovery. Genome Res. **6,** 791–806.

Brazma, A., et al. (2001). Minimum information about a microarray experiment (MIAME)-toward standards for microarray data. Nat. Genet. **29,** 365–371.

Brzobohaty, B., Moore, I., Kristoffersen, P., Bako, L., Campos, N., Schell, J., and Palme, K. (1993). Release of active cytokinin by a glucosidase localized to the maize root meristem. Science **262,** 1051–1054.

Bucher, M., Brunner, S., Zimmermann, P., Zardi, G.I., Amrhein, N., Willmitzer, L., and Riesmeier, J.W. (2002). The expression of an extensin-like protein correlates with cellular tip growth in tomato. Plant Physiol. **128,** 911–923.

Carpita, N.C., and Gibeaut, D.M. (1993). Structural models of primary

cell walls in flowering plants: Consistency of molecular structure with the physical properties of the walls during growth. Plant J. **3,** 1–30.

Cassab, G.I. (1998). Plant cell wall proteins. Annu. Rev. Plant Physiol. Plant Mol. Biol. **49,** 281–309.

Channelière, S., Rivière, S., Scalliet, G., Szecsi, J., Jullien, F., Dolle, C., Vergne, P., Dumas, C., Bendahmane, M., Hugueney, P., and Cock, J.M. (2002). Analysis of gene expression in rose petals using expressed sequence tags. FEBS Lett. **515,** 35–38.

Davies, B., Di Rosa, A., Eneva, T., Saedler, H., and Sommer, H. (1996). Alteration of tobacco floral organ identity by expression of combinations of *Antirrhinum* MADS-box genes. Plant J. **10,** 663–677.

Davis, L.L., and Bartnicki-Garcia, S. (1984). A model for the mechanism and regulation of chitosan synthesis in Mucor rouxii. In Structure, Function, and Biosynthesis of Plant Cell Walls, W.M. Dugger and S. Bartnicki-Garcia, eds (Rockville, MD: American Society of Plant Physiologists), pp. 400–408.

Draghici, S. (2003). Data Analysis Tools for DNA Microarrays. (London: Chapmann & Hall/CRC).

Dudareva, N., Murfitt, L.M., Mann, C.J., Gorenstein, N., Kolosova, N., Kish, C.M., Bonham, C., and Wood, K. (2000). Developmental regulation of methyl benzoate biosynthesis and emission in snapdragon flowers. Plant Cell **12,** 949–961.

Efremova, N., Perbal, M.C., Yephremov, A., Hofmann, W.A., Saedler, H., and Schwarz-Sommer, Z. (2001). Epidermal control of floral organ identity by class B homeotic genes in Antirrhinum and Arabidopsis. Development **128,** 2661–2671.

Egea-Cortines, M., Saedler, H., and Sommer, H. (1999). Ternary complex formation between the MADS-box proteins SQUAMOSA, DEFICIENS and GLOBOSA is involved in the control of floral architecture in Antirrhinum majus. EMBO J. **18,** 5370–5379.

Eisen, M.B., Spellman, P.T., Brown, P.O., and Botstein, D. (1998). Cluster analysis and display of genome-wide expression patterns. Proc. Natl. Acad. Sci. USA **95,** 14863–14868.

Fellenberg, K., Hauser, N.C., Brors, B., Hoheisel, J.D., and Vingron, M. (2002). Microarray data warehouse allowing for inclusion of experiment annotations in statistical analysis. Bioinformatics **18,** 423–433.

Fellenberg, K., Hauser, N.C., Brors, B., Neutzner, A., Hoheisel, J.D., and Vingron, M. (2001). Correspondence analysis applied to microarray data. Proc. Natl. Acad. Sci. USA **98,** 10781–10786.

Ferrario, S., Immink, R.G.H., Shchennikova, A., Busscher-Lange, J., and Angenent, G.C. (2003). The MADS box gene FBP2 is required for SEPALLATA function in petunia. Plant Cell **15,** 914–925.

Goto, K., and Meyerowitz, E.M. (1994). Function and regulation of the *Arabidopsis* floral homeotic gene *PISTILLATA*. Genes Dev. **8,** 1548–1560.

Guterman, I., et al. (2002). Rose scent: Genomics approach to discovering novel floral fragrance-related genes. Plant Cell **14,** 2325–2338.

Honma, T., and Goto, K. (2001). Complexes of MADS-box proteins are sufficient to convert leaves into floral organs. Nature **409,** 525–529.

Jack, T. (2004). Molecular and genetic mechanisms of floral control. Plant Cell **16 (suppl.),** S1–17.

Jack, T., Brockman, L.L., and Meyerowitz, E.M. (1992). The homeotic gene *APETALA3* of *Arabidopsis thaliana* encodes a MADS box and is expressed in petals and stamens. Cell **68,** 683–697.

Kieliszewski, M.J., and Lamport, D.T.A. (1994). Extensin: Repetitive motifs, functional sites, post-translational codes, and phylogeny. Plant J. **5,** 157–172.

Knox, P.J. (1995). Developmentally regulated proteoglycans and glycoproteins of the plant cell surface. FASEB J. **9,** 1004–1012.

Kopczak, S.D., Haas, N.A., Hussey, P.J., Silflow, C.D., and Snustad, D.P. (1992). The small genome of Arabidopsis contains at least six expressed alpha-tubulin genes. Plant Cell **4,** 539–547.

Kotilainen, M., Helariutta, Y., Elomaa, P., Paulin, L., and Teeri, T.H. (1994). A corolla- and carpel-abundant, non-specific lipid transfer protein gene is expressed in the epidermis and parenchyma of Gerbera hybrida var. Regina (Compositae). Plant Mol. Biol. **26,** 971–978.

Kotilainen, M., Helariutta, Y., Mehto, M., Pollanen, E., Albert, V.A., Elomaa, P., and Teeri, T.H. (1999). GEG participates in the regulation of cell and organ shape during corolla and carpel development in *Gerbera hybrida*. Plant Cell **11,** 1093–1104.

Lagorce, A., Hauser, N.C., Labourdette, D., Rodriguez, C., Martin-Yken, H., Arroyo, J., Hoheisel, J.D., and Francois, J. (2003). Genome-wide analysis of the response to cell wall mutations in the yeast *Saccharomyces cerevisiae*. J. Biol. Chem. **278,** 20345–20357.

Leinhos, V., Udagama-Randeniya, P.V., and Savidge, R.A. (1994). Purification of an acidic coniferin-hydrolysing beta-glucosidase from developing xylem of Pinus banksiana. Phytochemistry **37,** 311–315.

Liang, F., Holt, I., Pertea, G., Karamycheva, S., Salzberg, S.L., and Quackenbush, J. (2000). An optimized protocol for analysis of EST sequences. Nucleic Acids Res. **28,** 3657–3665.

Lohmann, J.U., and Weigel, D. (2002). Building beauty: The genetic control of floral patterning. Dev. Cell **2,** 135–142.

Luo, D., Carpenter, R., Copsey, L., Vincent, C., Clark, J., and Coen, E.S. (1999). Control of organ asymmetry in flowers of *Antirrhinum*. Cell **99,** 367–376.

Martin, C., and Gerats, T. (1993). Control of pigment biosynthesis genes during petal development. Plant Cell **5,** 1253–1264.

Mayer, U., and Jürgens, G. (2002). Microtubule cytoskeleton: A track record. Curr. Opin. Plant Biol. **5,** 494–501.

Nacken, W., Huijser, P., Saedler, H., and Sommer, H. (1991a). Molecular analysis of *tap2*, an anther-specific gene from *Antirrhinum majus*. FEBS Lett. **280,** 155–158.

Nacken, W., Huijser, P., Saedler, H., and Sommer, H. (1991b). Molecular characterisation of two stamen-specific genes, *tap1* and *tap2*, that are expressed in the wild type, but not in *deficiens* mutant of *Antirrhinum majus*. Mol. Gen. Genet. **229,** 129–136.

Noda, K., Glover, B.J., Linstead, P., and Martin, C. (1994). Flower colour intensity depends on specialized cell shape controlled by a Myb-related transcription factor. Nature **369,** 661–664.

Perbal, M.C., Haughn, G., Saedler, H., and Schwarz-Sommer, Z. (1996). Non-cell-autonomous function of the Antirrhinum floral homeotic proteins DEFICIENS and GLOBOSA is exerted by their polar cell-to-cell trafficking. Development **122,** 3433–3441.

Pichersky, E., and Gang, D.R. (2000). Genetics and biochemistry of secondary metabolites in plants: An evolutionary perspective. Trends Plant Sci. **5,** 439–445.

Pyke, K.A., and Page, A.M. (1998). Plastid ontogeny during petal development in Arabidopsis. Plant Physiol. **116,** 797–803.

Rolland-Lagan, A.-G., Bangham, J.A., and Coen, E.S. (2003). Growth dynamics underlying petal shape and asymmetry. Nature **422,** 161–163.

Rubinelli, P., Hu, Y., and Ma, H. (1998). Identification, sequence analysis and expression studies of novel anther-specific genes of Arabidopsis thaliana. Plant Mol. Biol. **37,** 607–619.

Sablowski, R.W.M., and Meyerowitz, E.M. (1998). A homolog of *NO APICAL MERISTEM* is an immediate target of the floral homeotic genes *APETALA3*/*PISTILLATA*. Cell **92,** 93–103.

Samach, A., Kohalmi, S.E., Motte, P., Datla, R., and Haughn, G. (1997). Divergence of function and regulation of class B floral organ identity genes. Plant Cell **9,** 559–570.

Schäffner, A.R. (1998). Aquaporin function, structure, and expression: Are there more surprises to surface in water relations? Planta **204,** 131–139.

Schmid, M., Uhlenhaut, N.H., Godard, F., Demar, M., Bressan, R., Weigel, D., and Lohmann, J.U. (2003). Dissection of floral induction

pathways using global expression analysis. Development **130,** 6001–6012.

Schratt, G., Philippar, U., Berger, J., Schwarz, H., Heidenreich, O., and Nordheim, A. (2002). Serum response factor is crucial for actin cytoskeletal organization and focal adhesion assembly in embryonic stem cells. J. Cell Biol. **156,** 737–750.

Schwarz-Sommer, Z., Davies, B., and Hudson, A. (2003). An everlasting pioneer: The story of *Antirrhinum* research. Nat. Rev. Genet. **4,** 657–666.

Schwarz-Sommer, Z., Hue, I., Huijser, P., Flor, P., Hansen, H., Tetens, F., Lönnig, W.E., Saedler, H., and Sommer, H. (1992). Characterization of the Antirrhinum floral homeotic MADS-box gene deficiens: Evidence for DNA-binding and autoregulation of its persistent expression throughout flower development. EMBO J. **11,** 251–263.

Sommer, H., Beltran, P., Huijser, P., Pape, H., Lönnig, W.E., Saedler, H., and Schwarz-Sommer, Z. (1990). Deficiens, a homeotic gene involved in the control of flower morphogenesis in *Antirrhinum majus*: The protein shows homology to transcription factors. EMBO J. **9,** 605–613.

Sue, M., Ishihara, A., and Iwamura, H. (2000). Purification and characterization of a hydroxamic acid glucoside β-glucosidase from wheat (Triticum aestivum L.) seedlings. Planta **210,** 432–438.

Thoma, S., Kaneko, Y., and Somerville, C. (1993). A non-specific lipid transfer protein from Arabidopsis is a cell wall protein. Plant J. **3,** 427–436.

Tröbner, W., Raminez, L., Motte, P., Hue, I., Huijser, P., Lönnig, W.E., Saedler, H., Sommer, H., and Schwarz-Sommer, Z. (1992). GLOBOSA: A homeotic gene which interacts with DEFICIENS in the control of Antirrhinum floral organogenesis. EMBO J. **11,** 4693–4704.

Upton, C., and Buckley, J.T. (1995). A new family of lipolytic enzymes? Trends Biochem. Sci. **20,** 178–179.

van Doorn, W.G., Balk, P.A., van Houwelingen, A.M., Hoeberichts, F.A., Hall, R.D., Vorst, O., van der Schoot, C., and van Wordragen, M.F. (2003). Gene Expression during anthesis and senescence in *Iris* flowers. Plant Mol. Biol. **53,** 845–863.

Vincent, C.A., and Coen, E.S. (2004). A temporal and morphological framework for flower development in *Antirrhinum majus*. Can. J. Bot. **84,** 681–690.

Wellmer, F., Riechmann, J.L., Alves-Ferreira, M., and Meyerowitz, E.M. (2004). Genome-wide analysis of spatial gene expression in Arabidopsis flowers. Plant Cell **16,** 1314–1326.

Werneke, J.M., Chatfield, J.M., and Ogren, W.L. (1989). Alternative mRNA splicing generates the two ribulosebisphosphate carboxylase/oxygenase activase polypeptides in spinach and Arabidopsis. Plant Cell **1,** 815–825.

Wilmouth, R.C., Turnbull, J.J., Welford, R.W.D., Clifton, I.J., Prescott, A.G., and Schofield, C.J. (2002). Structure and mechanism of anthocyanidin synthase from Arabidopsis thaliana. Structure **10,** 93–103.

Zachgo, S. (2002). *In situ* hybridization. In Molecular Plant Biology, P.M. Gilmartin and C. Bowler, eds (Oxford, UK: Oxford University Press), pp. 41–63.

Zachgo, S., de Andrade Silva, E., Motte, P., Tröbner, W., Saedler, H., and Schwarz-Sommer, Z. (1995). Functional analysis of the *Antirrhinum* floral homeotic *DEFICIENS* gene *in vivo* and *in vitro* by using a temperature-sensitive mutant. Development **121,** 2861–2875.

Zachowski, A., Guerbette, F., Grosbois, M., Jolliot-Croquin, A., and Kader, J.C. (1998). Characterisation of acyl binding by a plant lipid-transfer protein. Eur. J. Biochem. **257,** 443–448.

Zielinski, R.E. (1998). Calmodulin and calmodulin-binding proteins in plants. Annu. Rev. Plant Physiol. Plant Mol. Biol. **49,** 697–725.

Zik, M., and Irish, V.F. (2003). Global identification of target genes regulated by *APETALA3* and *PISTILLATA* floral homeotic gene action. Plant Cell **15,** 207–222.